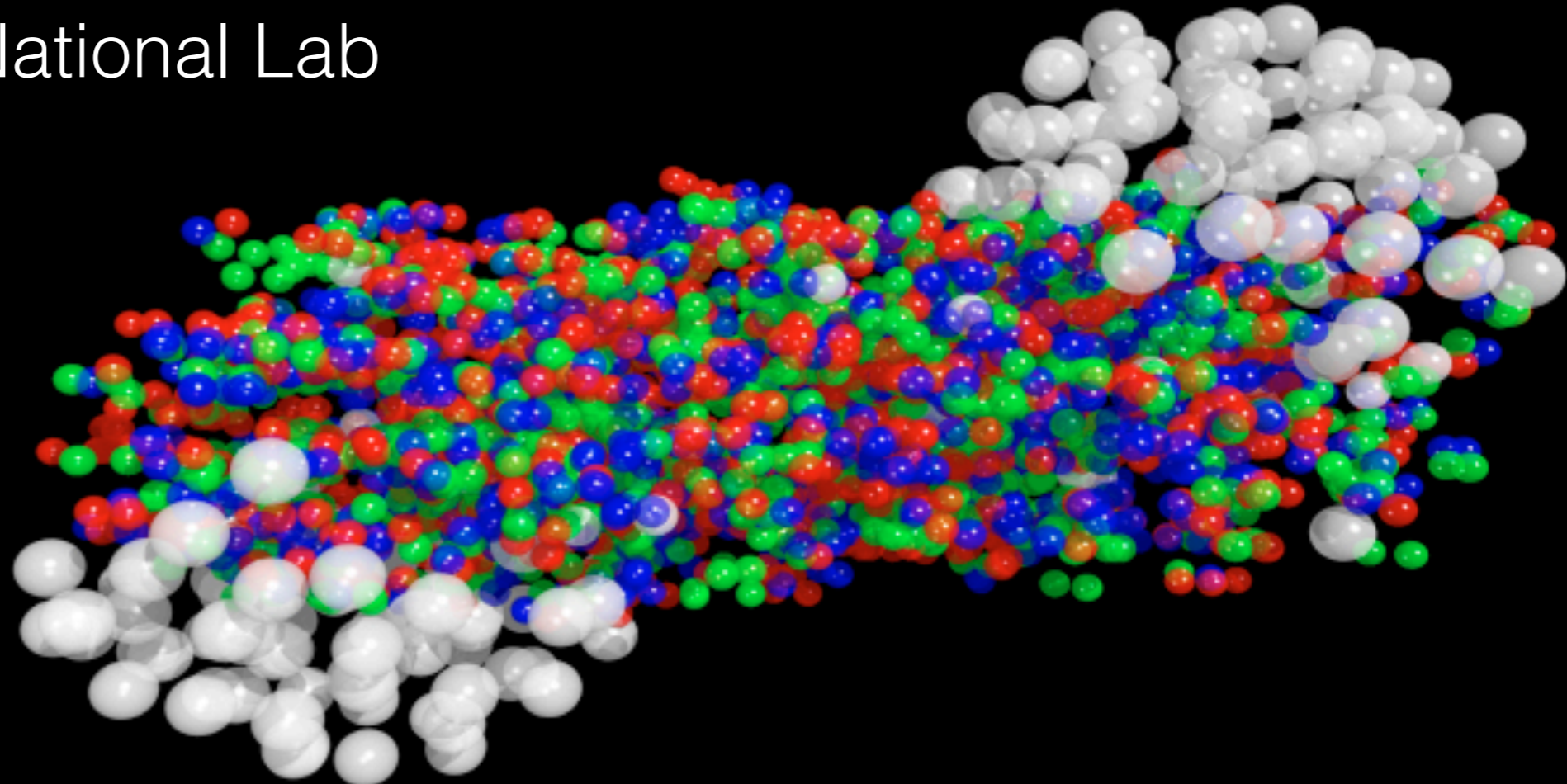


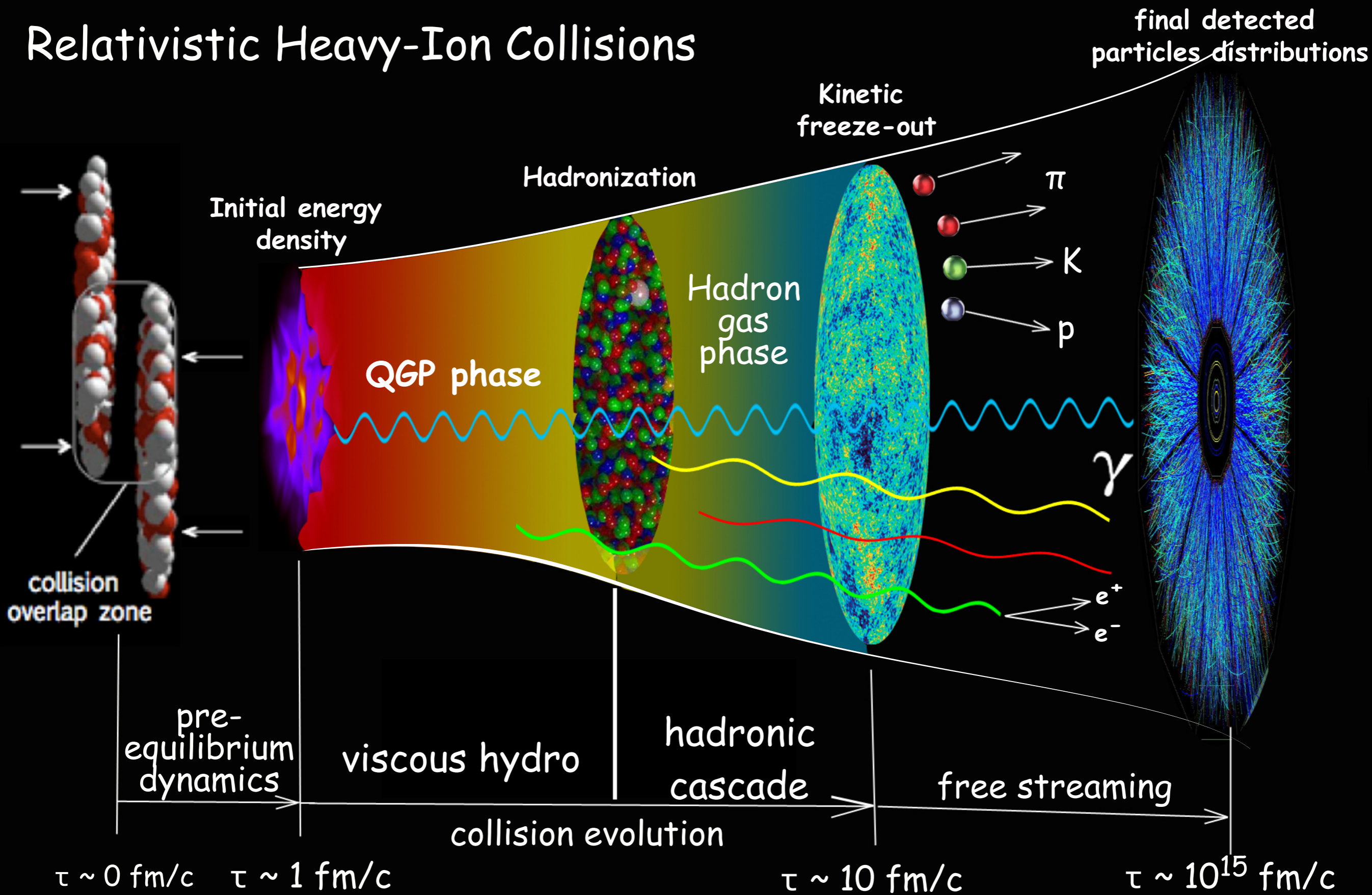
Hydrodynamic Simulations for the RHIC-BES, Progress, and Challenges

Chun Shen

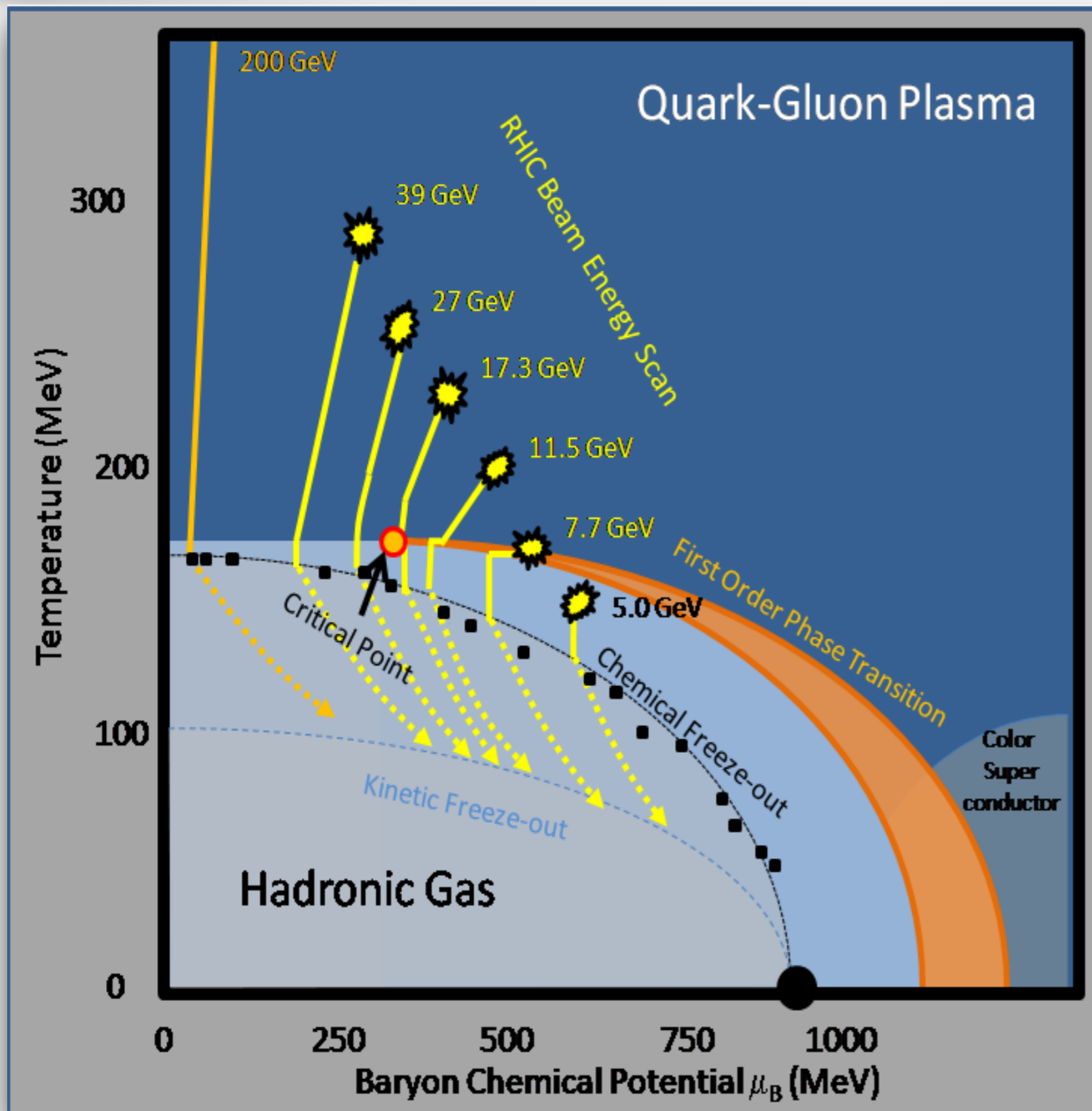
Brookhaven National Lab



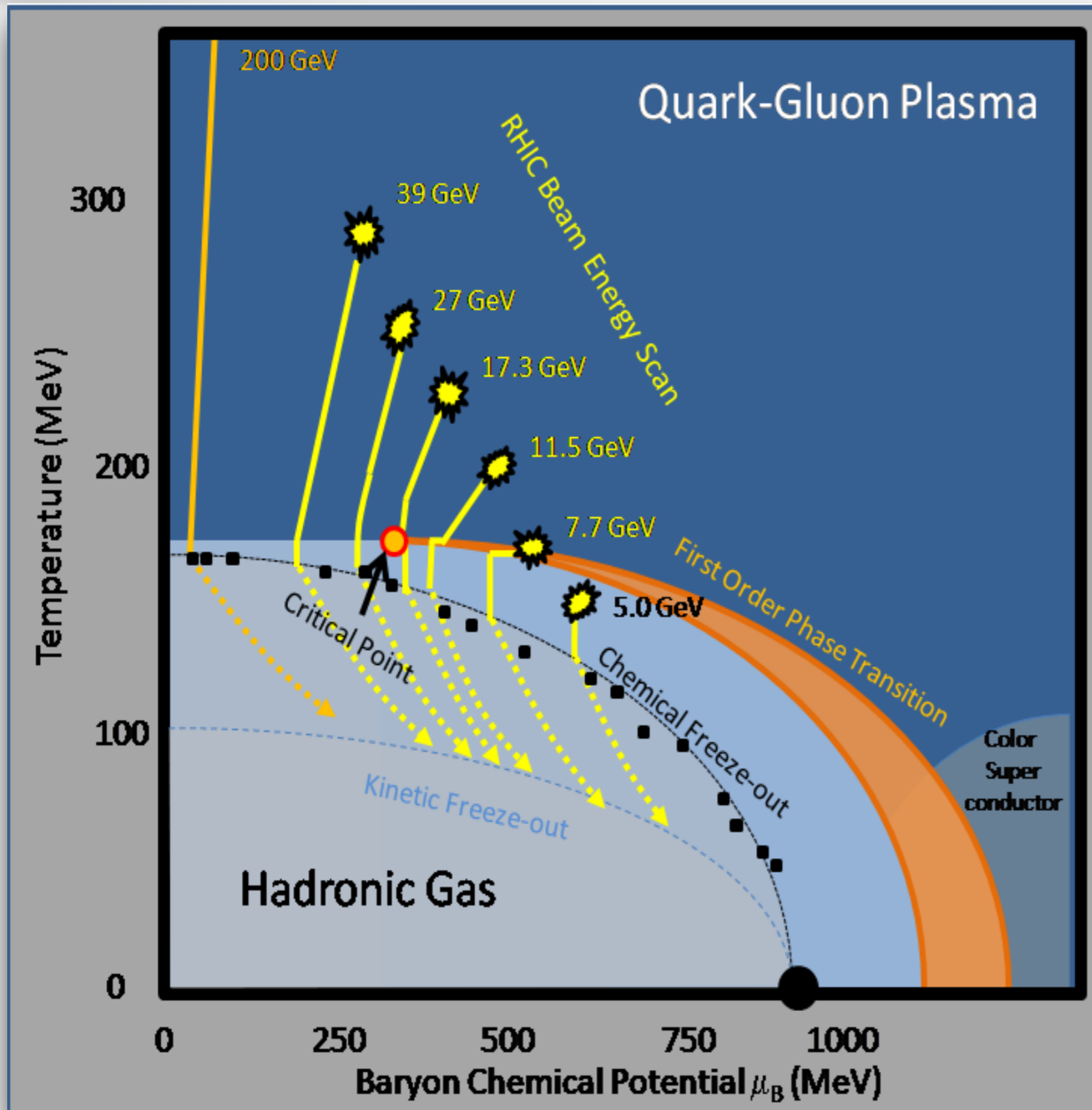
Relativistic Heavy-Ion Collisions



Exploring the phases of QCD

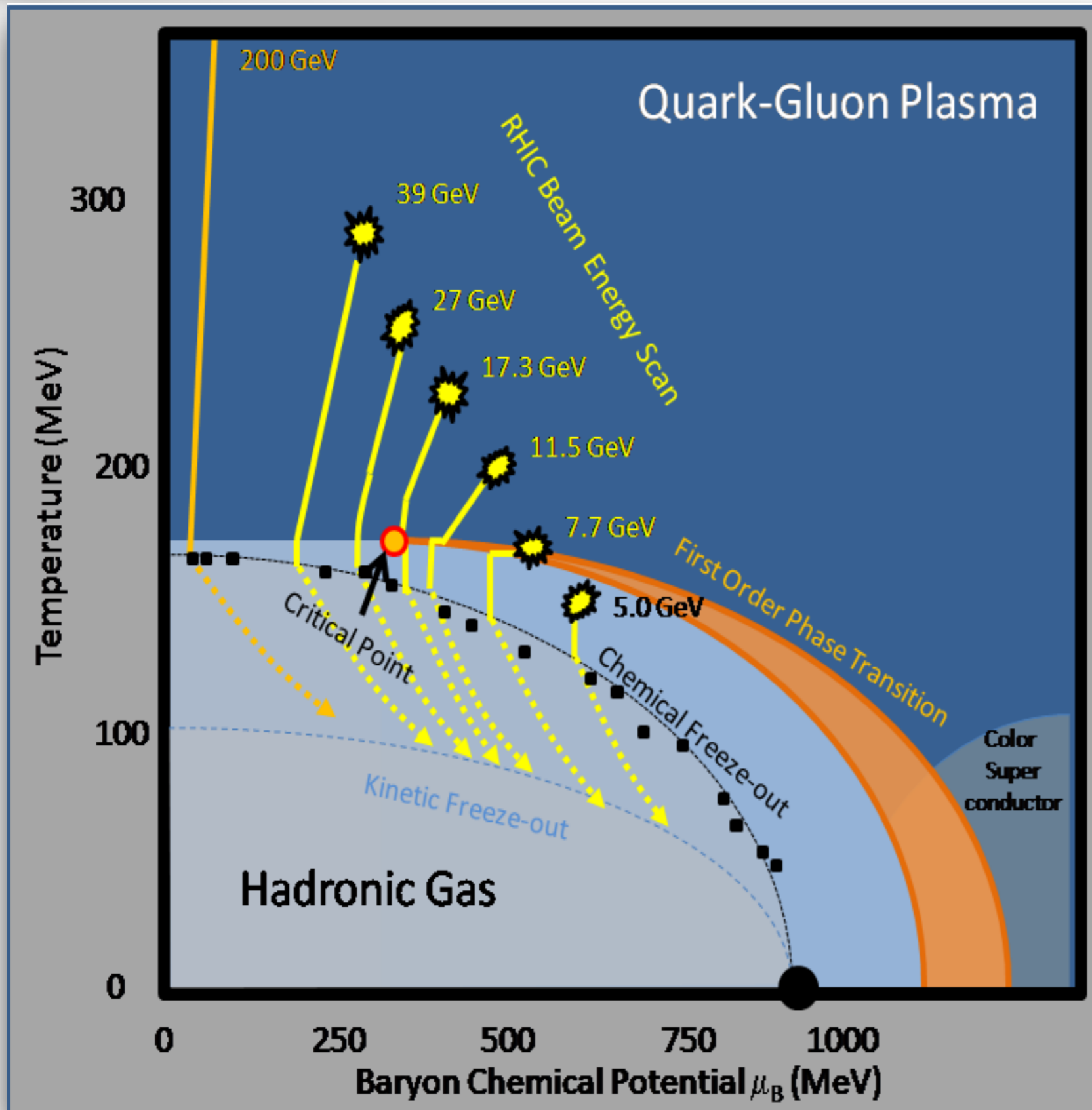


Exploring the phases of QCD



- Event-by-event fluctuating initial conditions
- (3+1)-d dissipative hydrodynamic modelling of the QGP
- Microscopic description for hadronic phase

Exploring the phases of QCD



- Event-by-event fluctuating initial conditions

Glauber-LEXUS

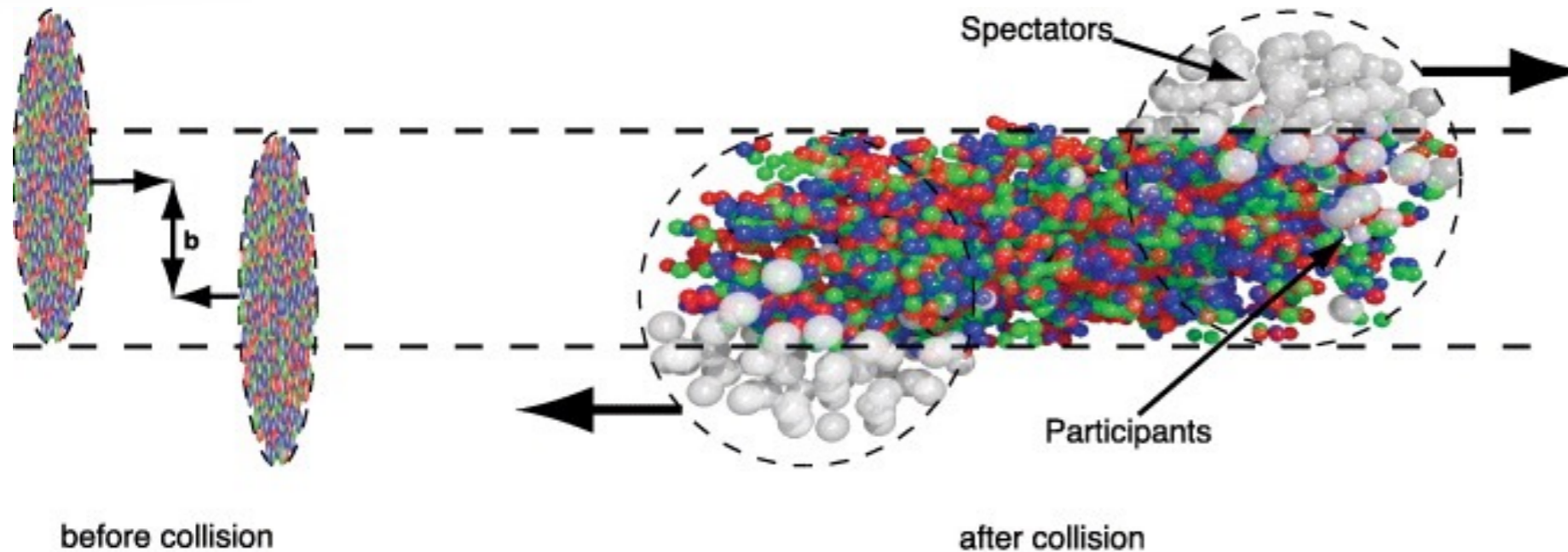
- (3+1)-d dissipative hydrodynamic modelling of the QGP

MUSIC

- Microscopic description for hadronic phase

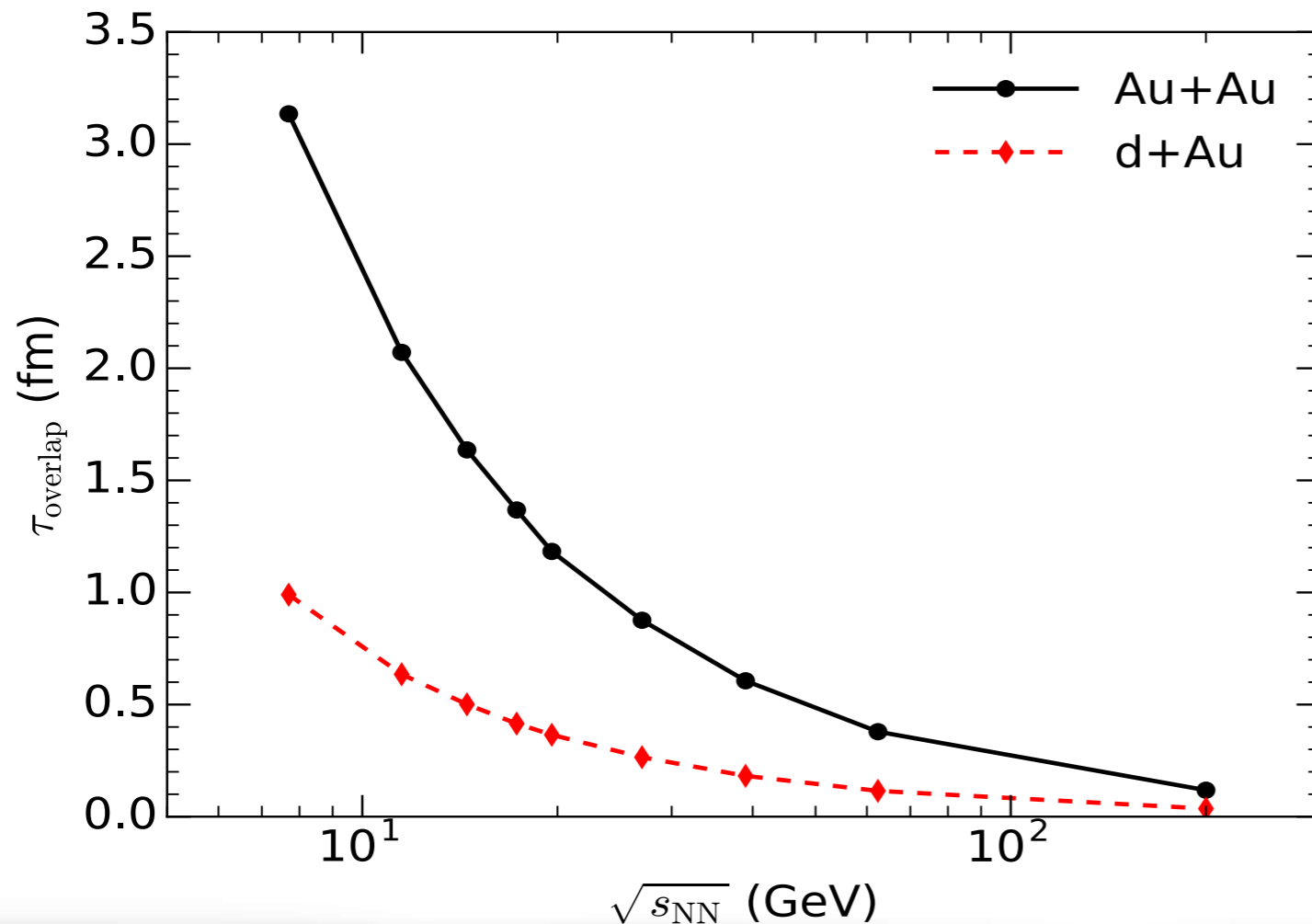
UrQMD/JAM

When to start hydrodynamics?



Two nuclei
overlapping time

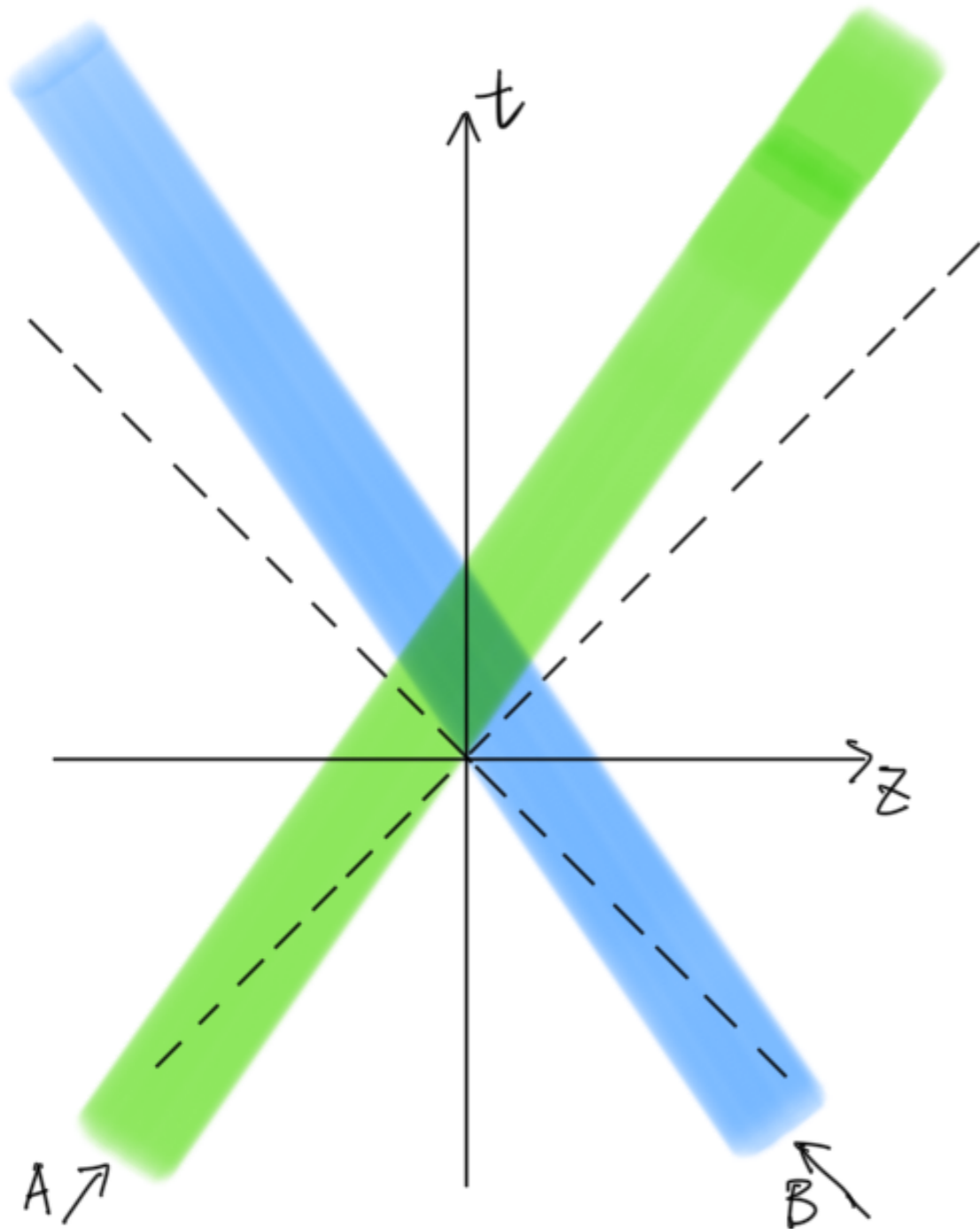
$$\tau \sim \frac{2R}{\gamma v_z}$$



- Nuclei overlapping time is **large** at low collision energy
- **Pre-equilibrium dynamics** can play an important role

Go beyond the Bjorken approximation

- The finite widths of the colliding nuclei are taken into account

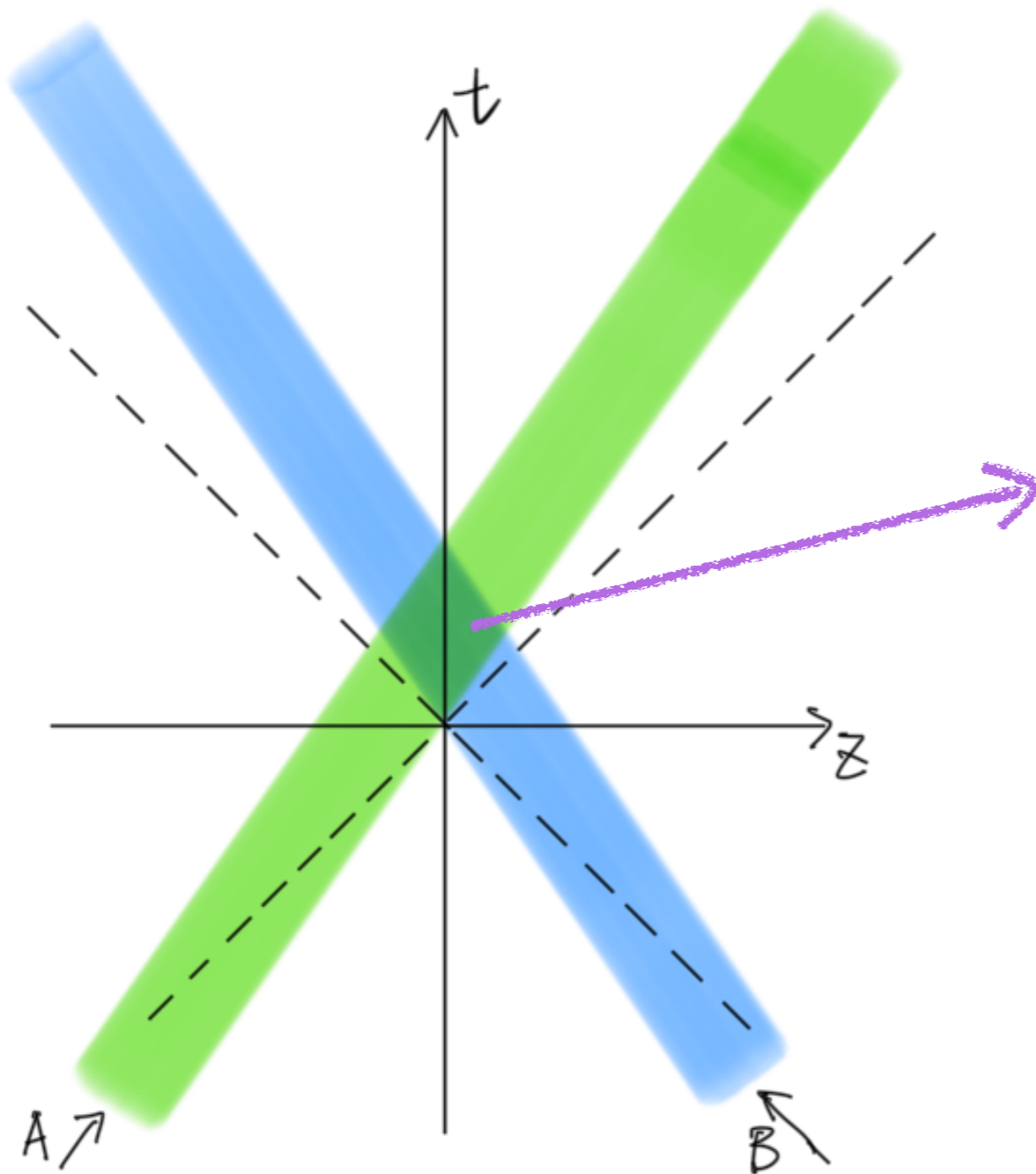


Go beyond the Bjorken approximation

- The finite widths of the colliding nuclei are taken into account

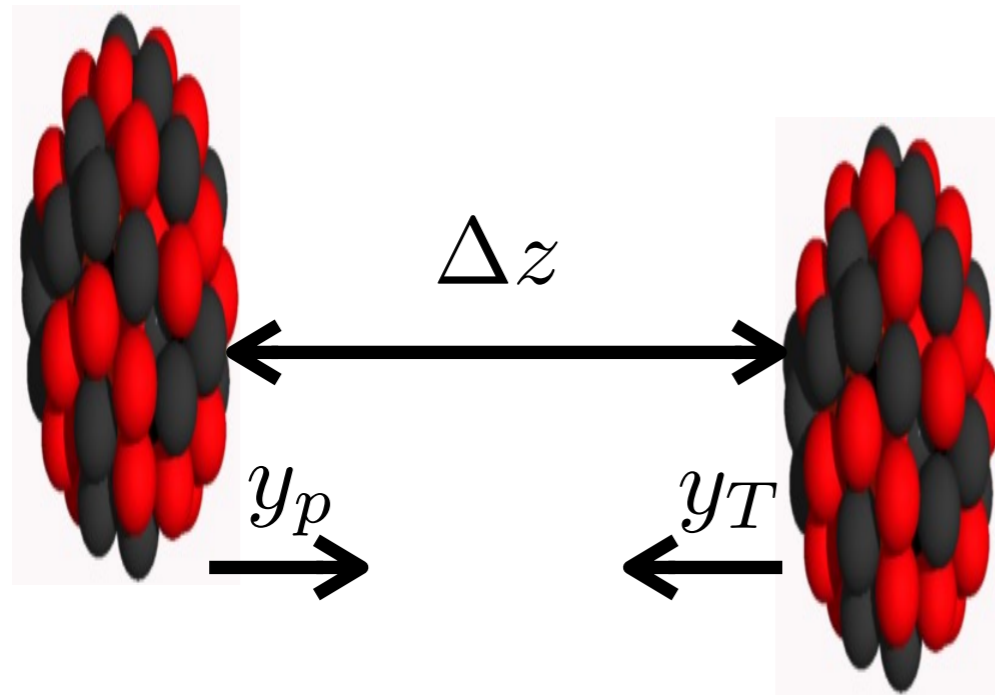
The interaction zone is not point like

$$y \neq \eta_s$$



The 3D MCGlauber-LEXUS model

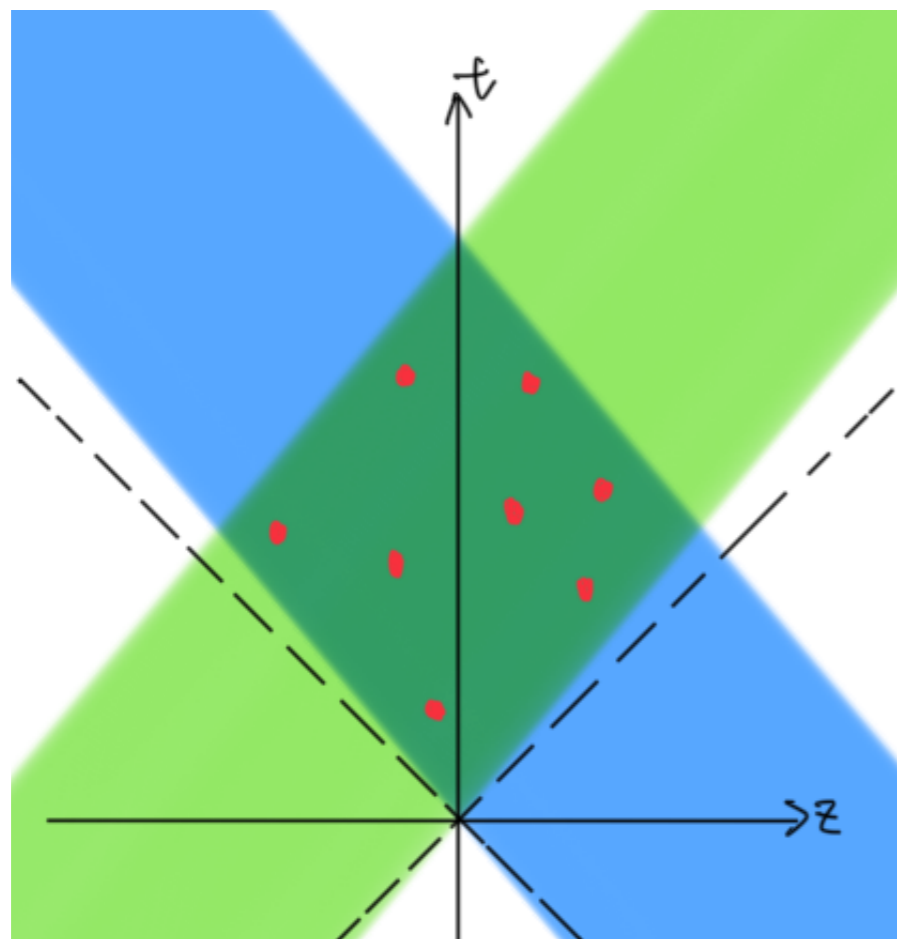
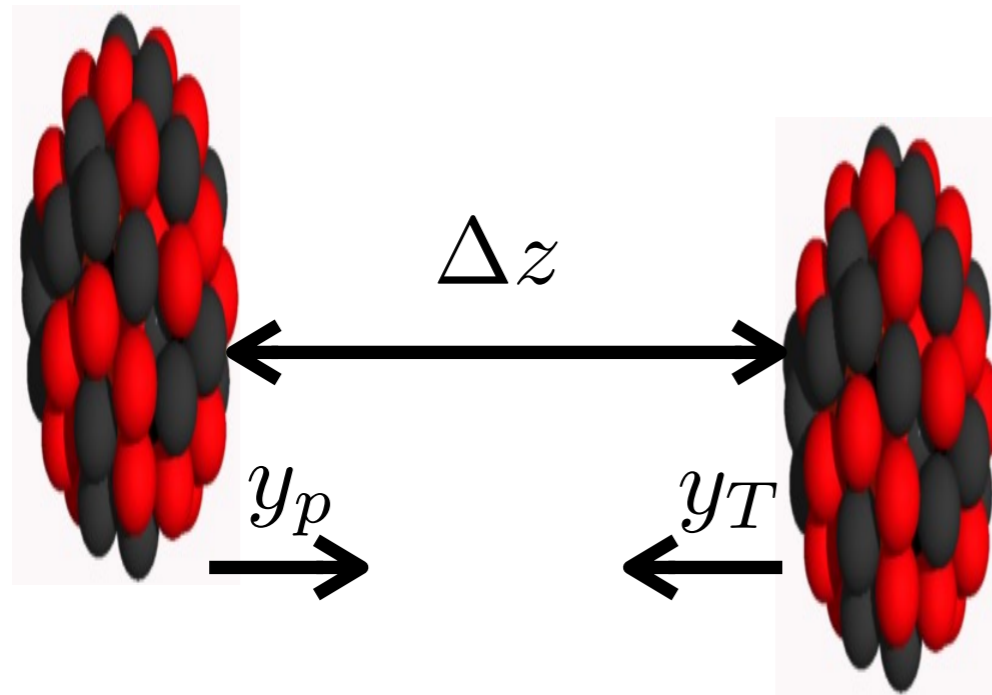
C. Shen, B. Schenke, in preparation



- Collision time and 3D spatial position are determined for every binary collision

A 3D MCGlauber model

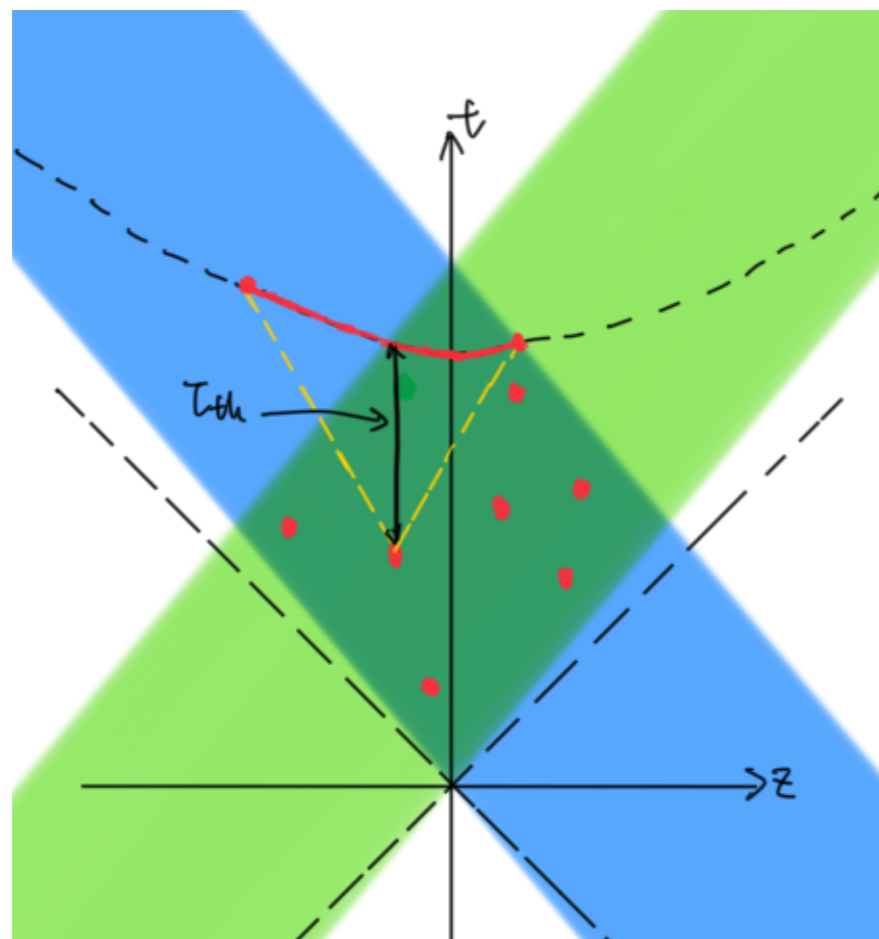
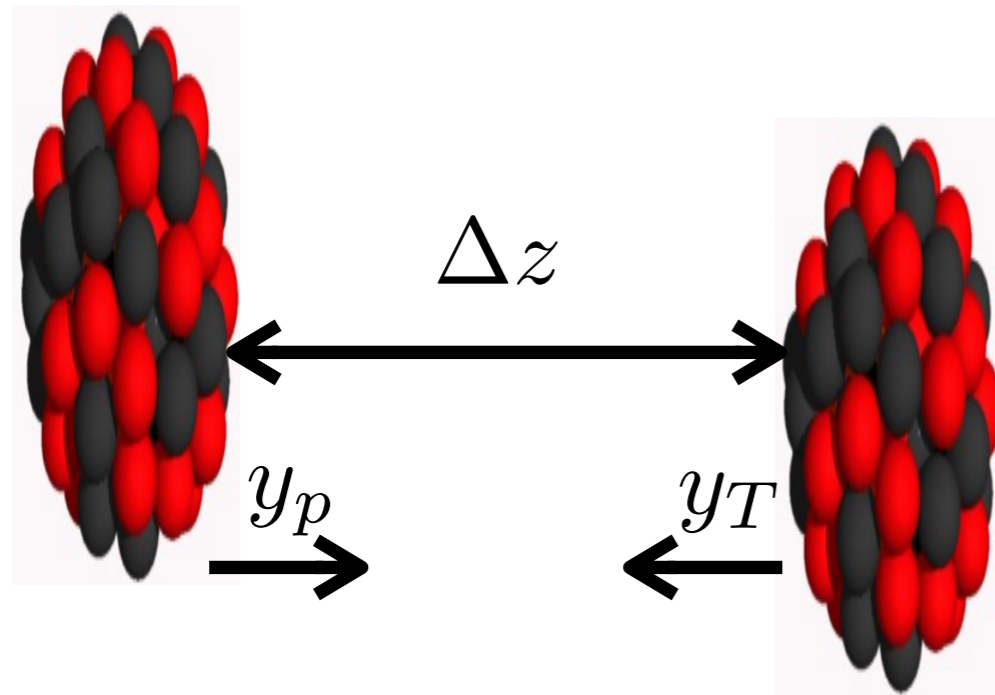
C. Shen, B. Schenke, in preparation



- Collision time and 3D spatial position are determined for every binary collision
- QCD strings are randomly produced from collision points

A 3D MCGlauber model

C. Shen, B. Schenke, in preparation



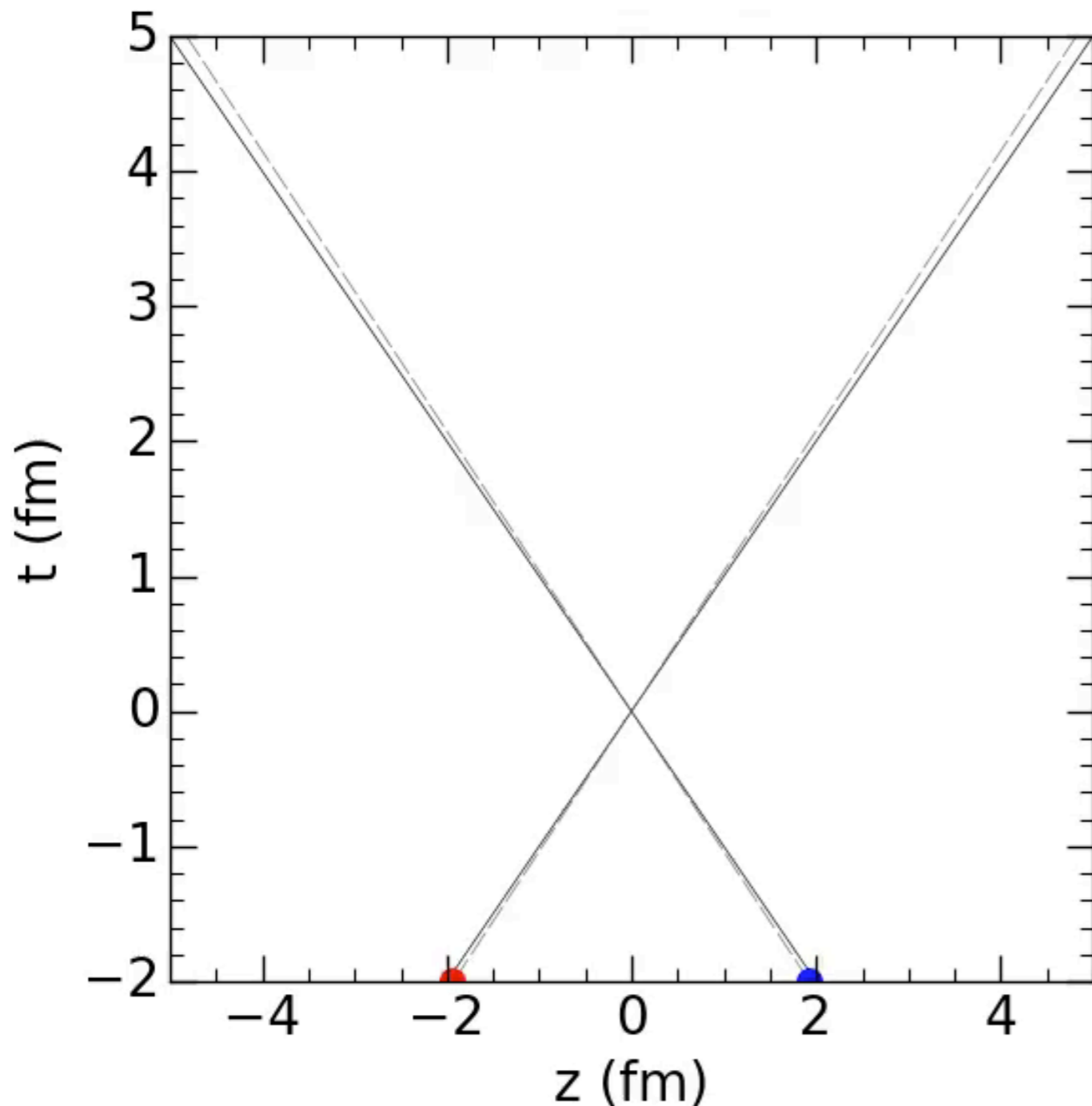
- Collision time and 3D spatial position are determined for every binary collision
- QCD strings are randomly produced from collision points

A. Bialas, A. Bzdak and V. Koch,
arXiv:1608.07041 [hep-ph]

- These strings are decelerated with a constant string tension $\sigma = 1 \text{ GeV}/\text{fm}$ before thermalized to medium

The 3D MCGlauber-LEXUS model

C. Shen, B. Schenke, in preparation



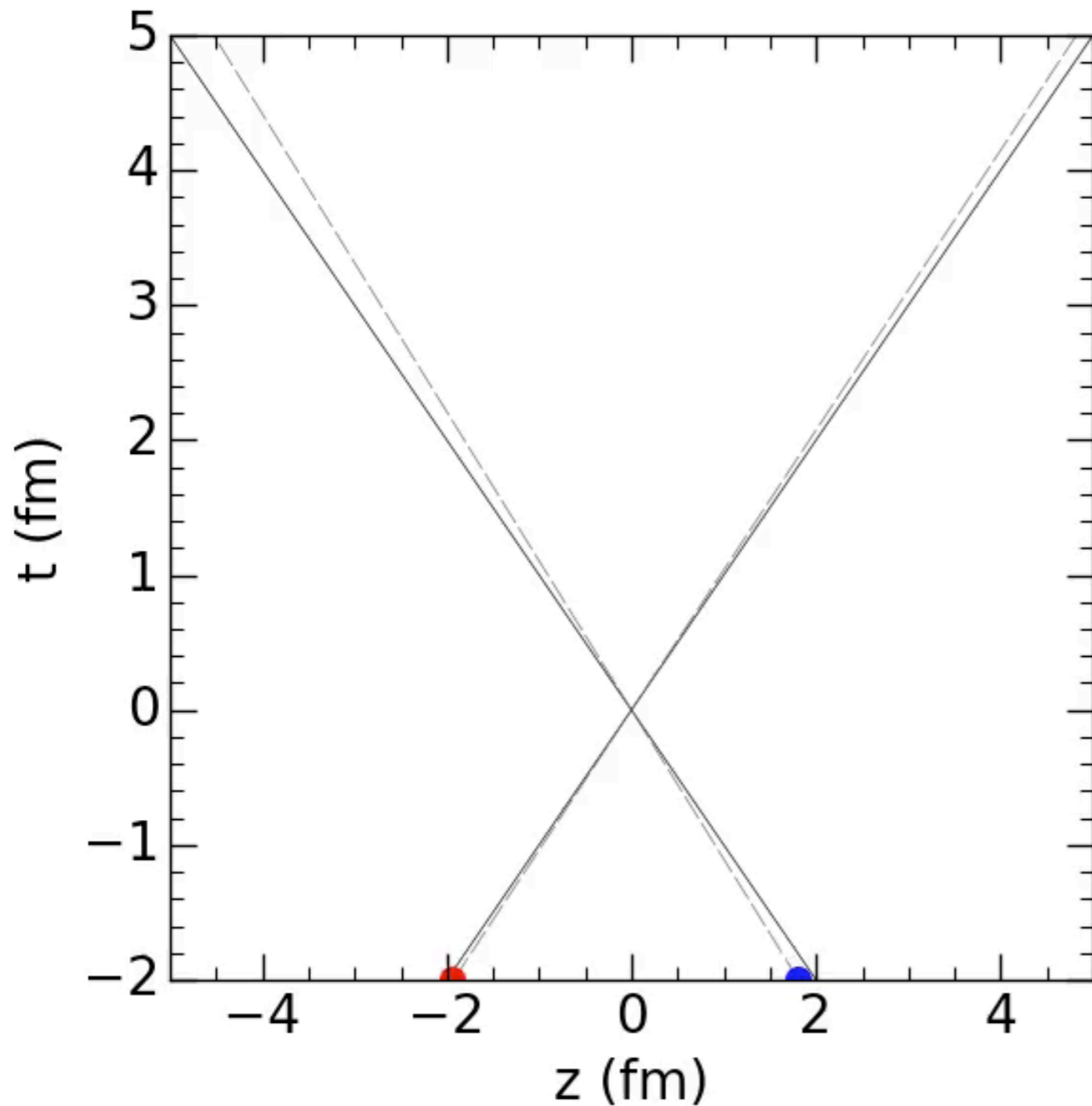
- Collision time and 3D spatial position are determined for every binary collision
- QCD strings are randomly produced from collision points

A. Bialas, A. Bzdak and V. Koch,
arXiv:1608.07041 [hep-ph]

- These strings are decelerated with a constant string tension $\sigma = 1 \text{ GeV}/\text{fm}$ before thermalized to medium

The 3D MCGlauber-LEXUS model

C. Shen, B. Schenke, in preparation



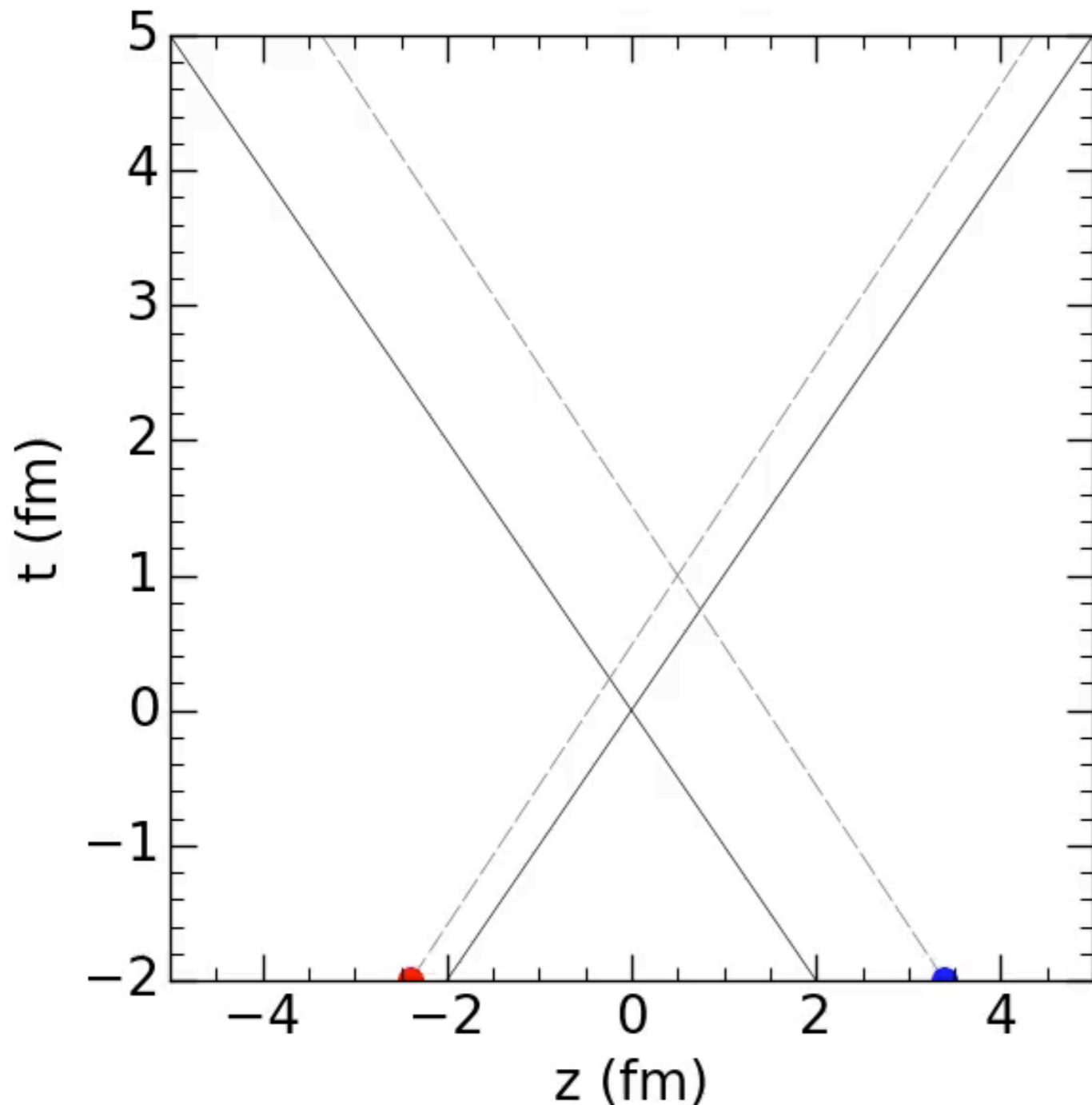
- Collision time and 3D spatial position are determined for every binary collision
- QCD strings are randomly produced from collision points

A. Bialas, A. Bzdak and V. Koch,
arXiv:1608.07041 [hep-ph]

- These strings are decelerated with a constant string tension $\sigma = 1 \text{ GeV}/\text{fm}$ before thermalized to medium

The 3D MCGlauber-LEXUS model

C. Shen, B. Schenke, in preparation

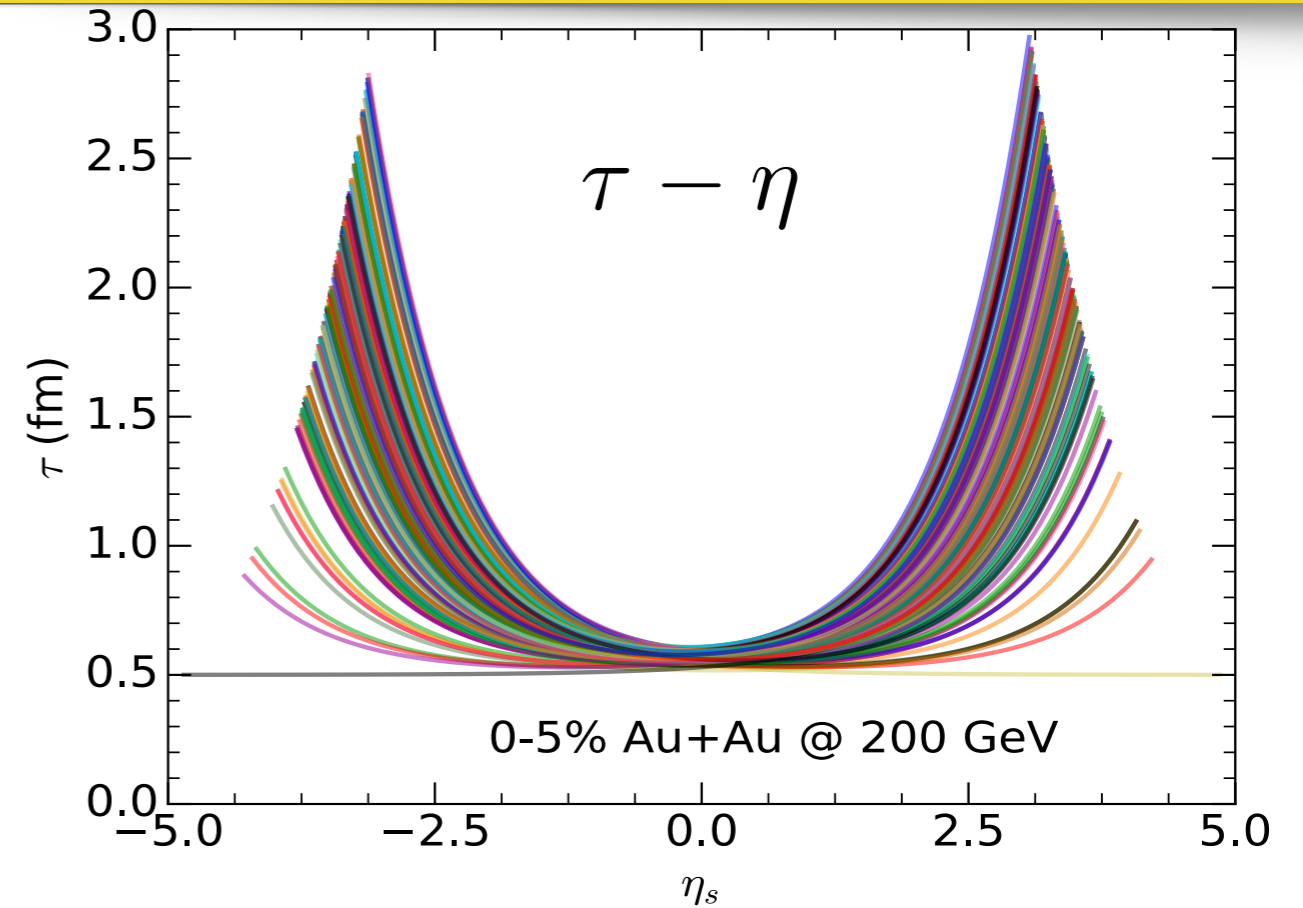
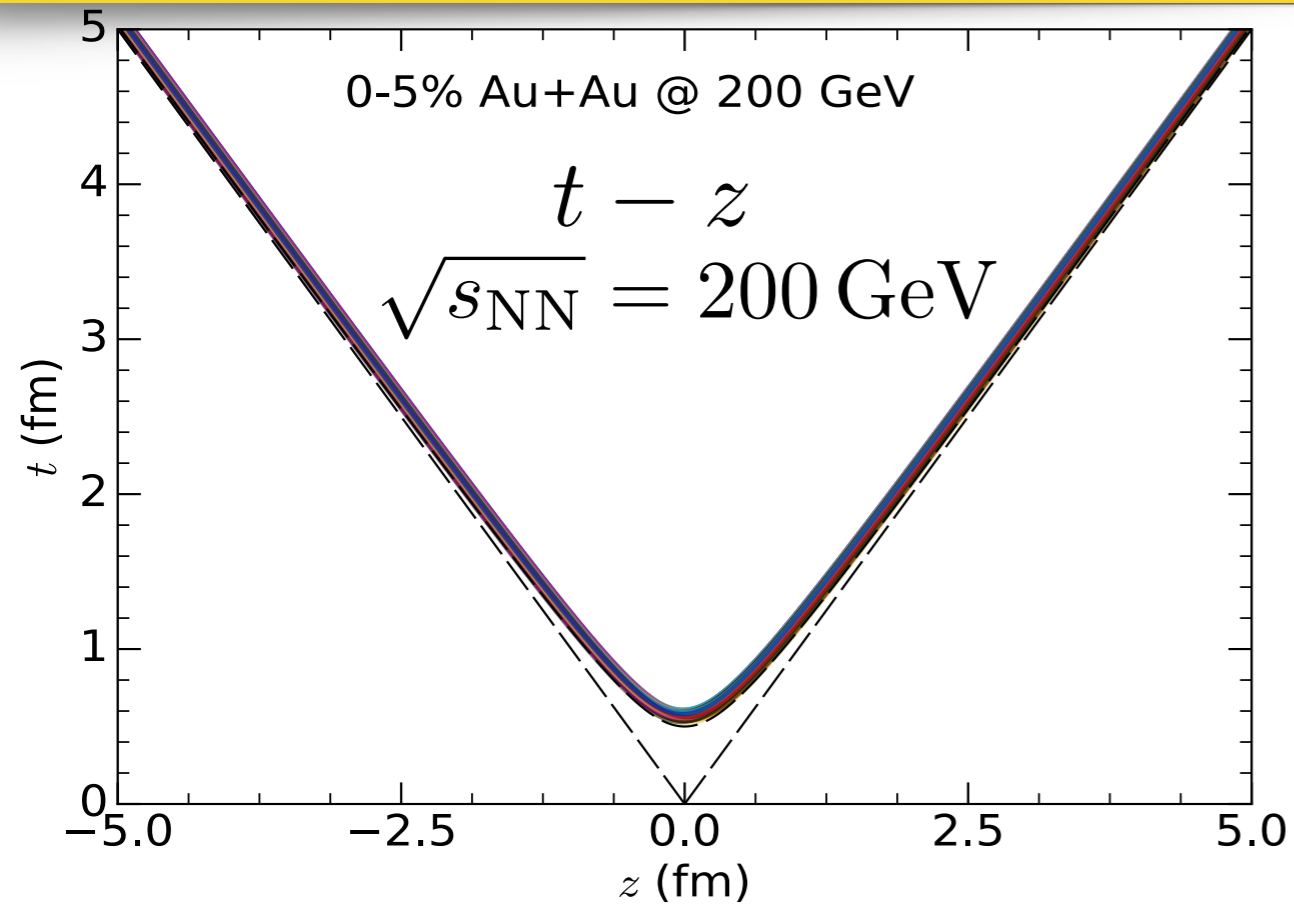


- Collision time and 3D spatial position are determined for every binary collision
- QCD strings are randomly produced from collision points

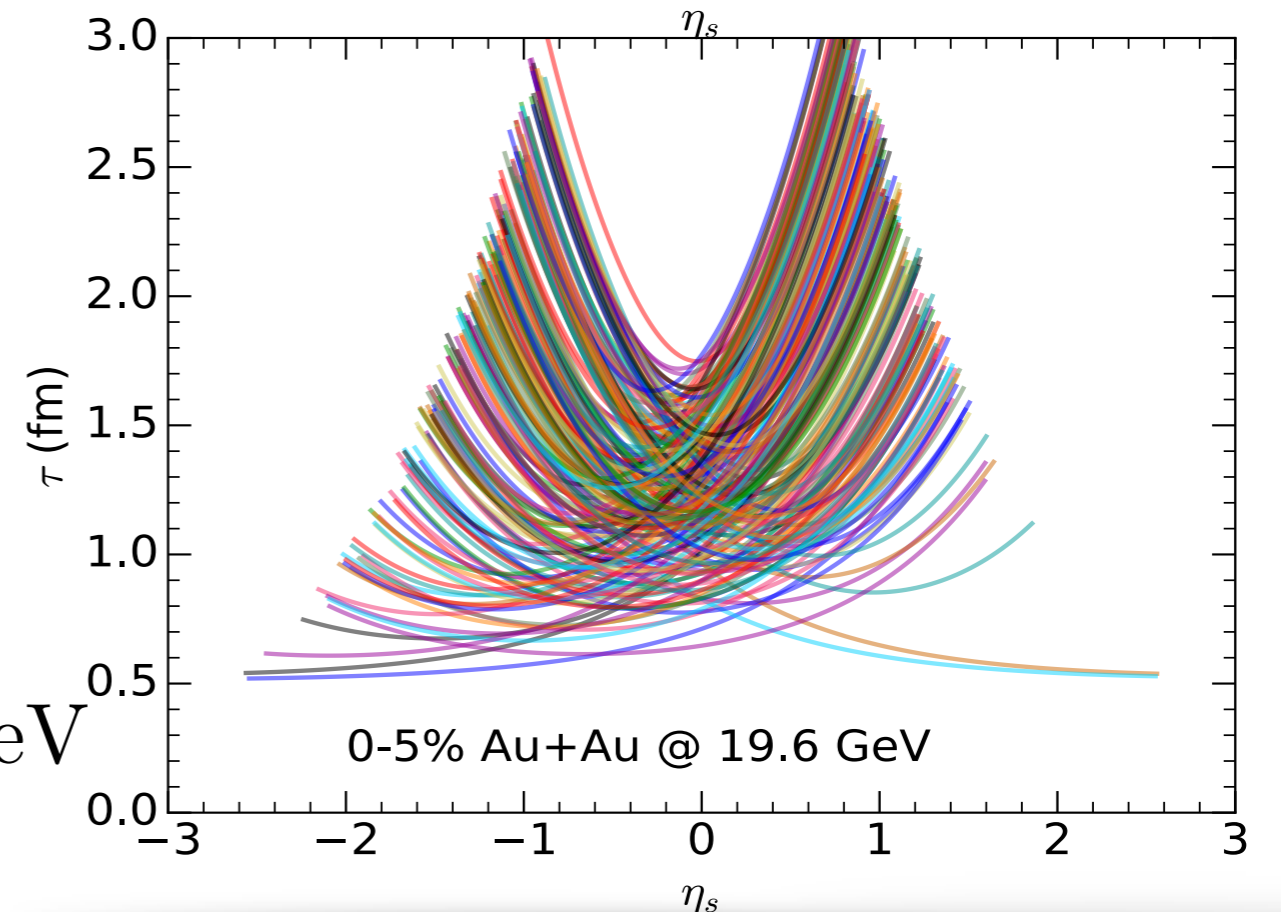
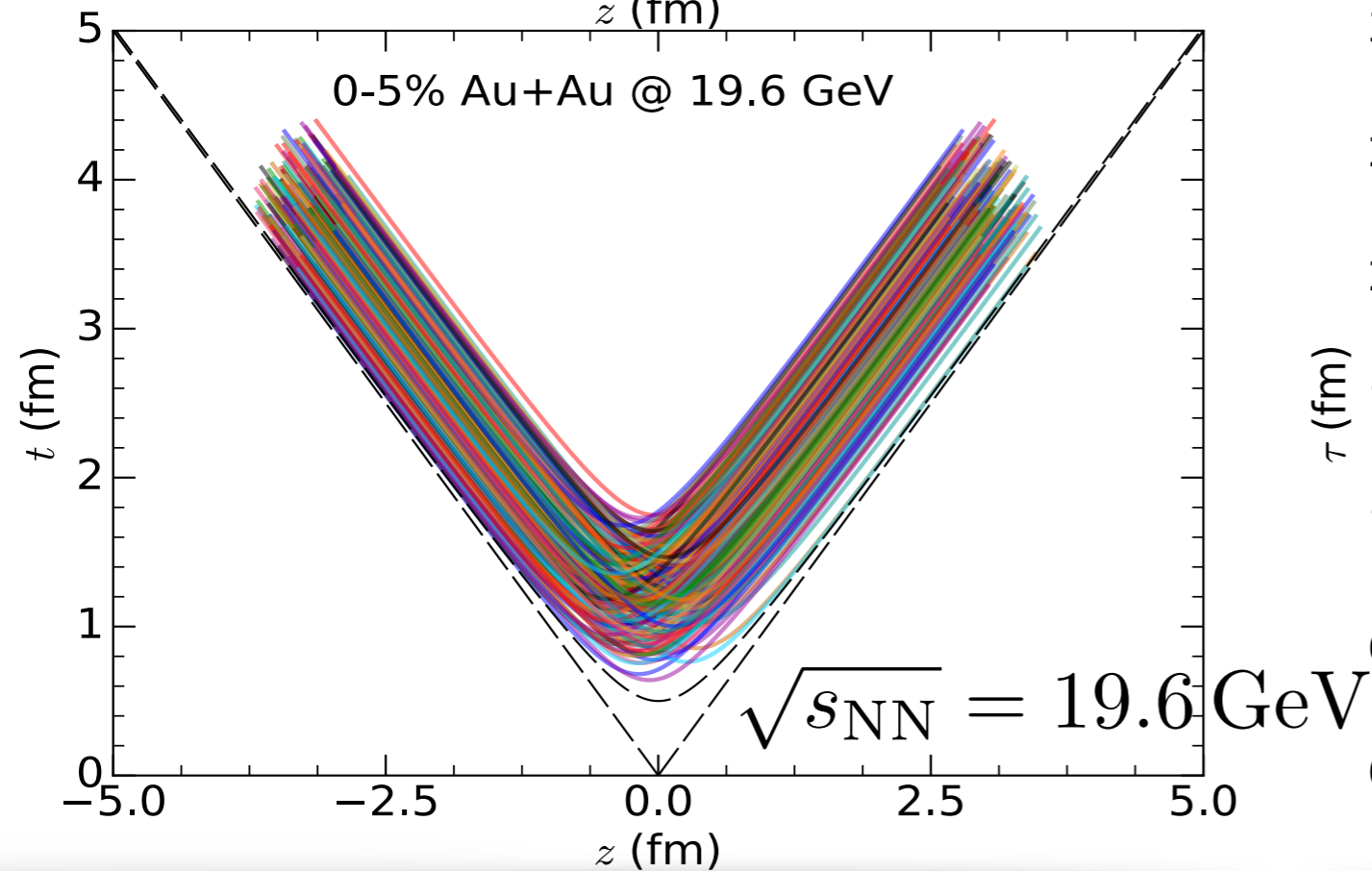
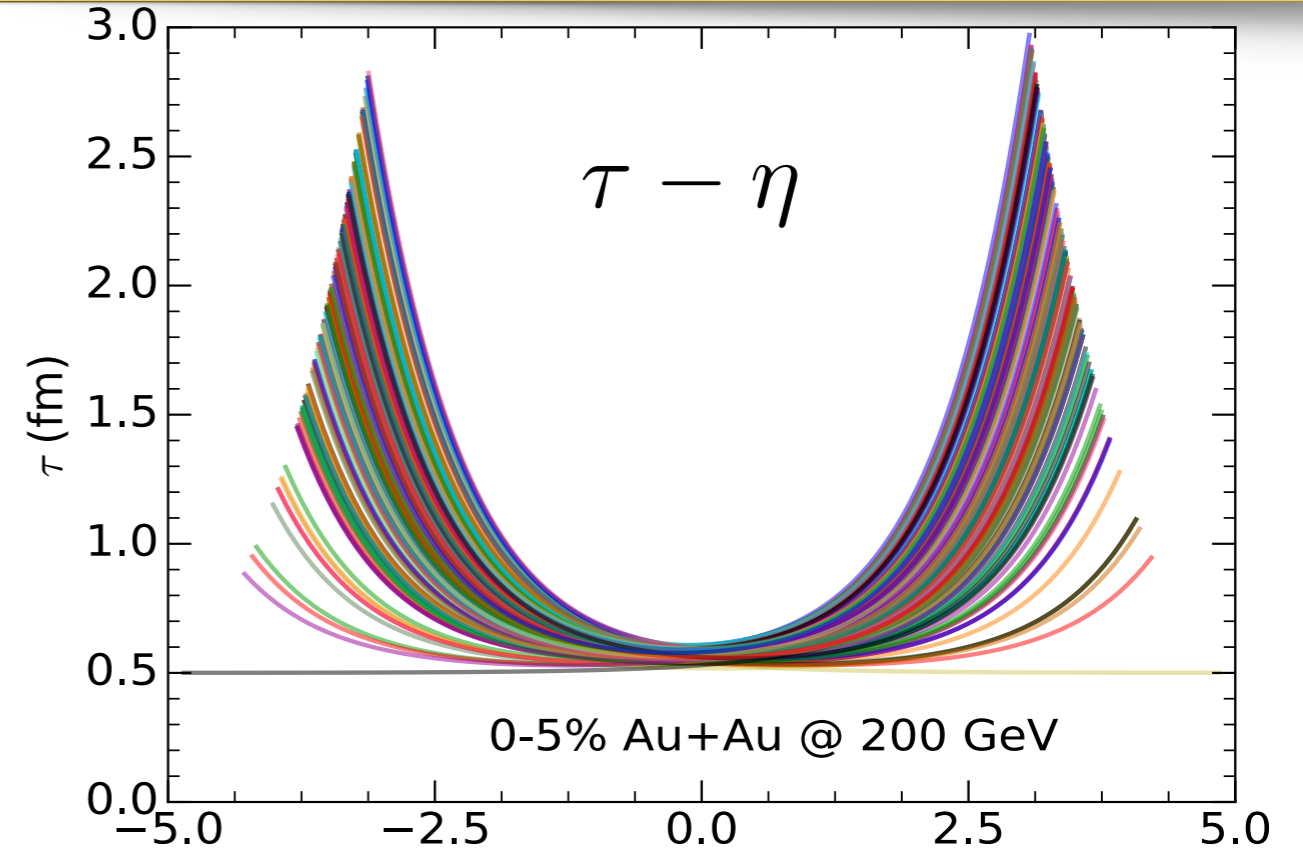
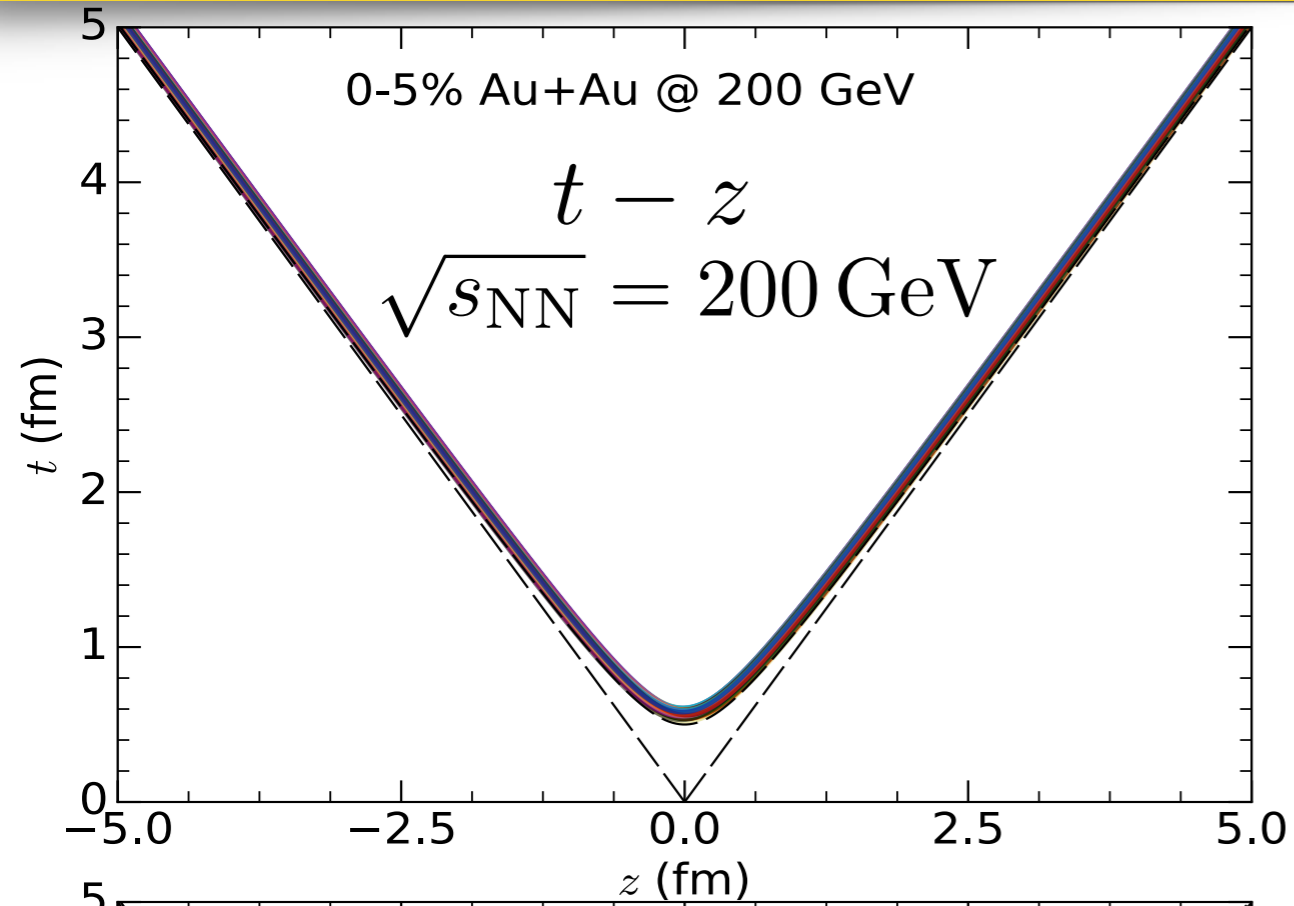
A. Bialas, A. Bzdak and V. Koch,
arXiv:1608.07041 [hep-ph]

- These strings are decelerated with a constant string tension $\sigma = 1 \text{ GeV}/\text{fm}$ before thermalized to medium

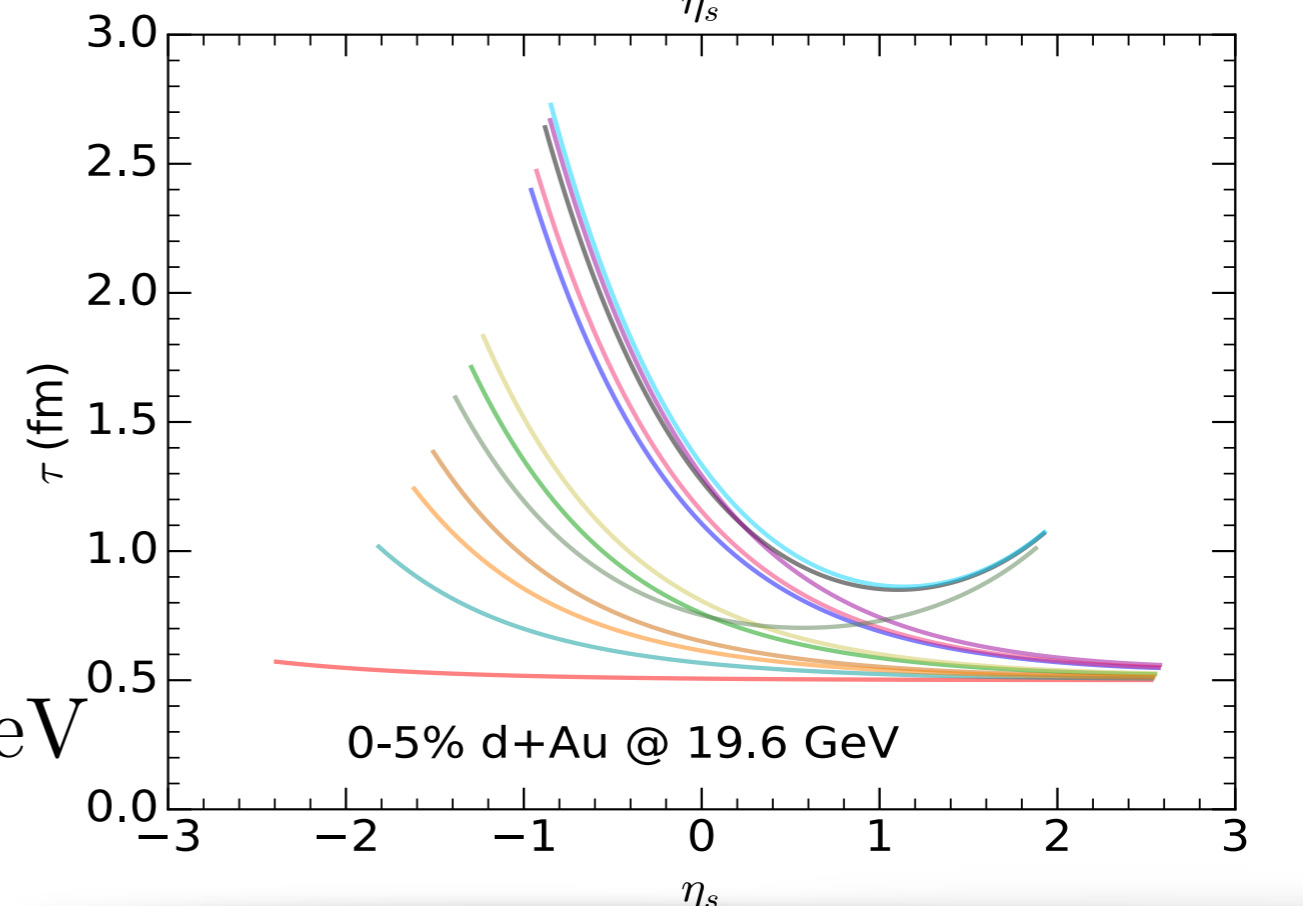
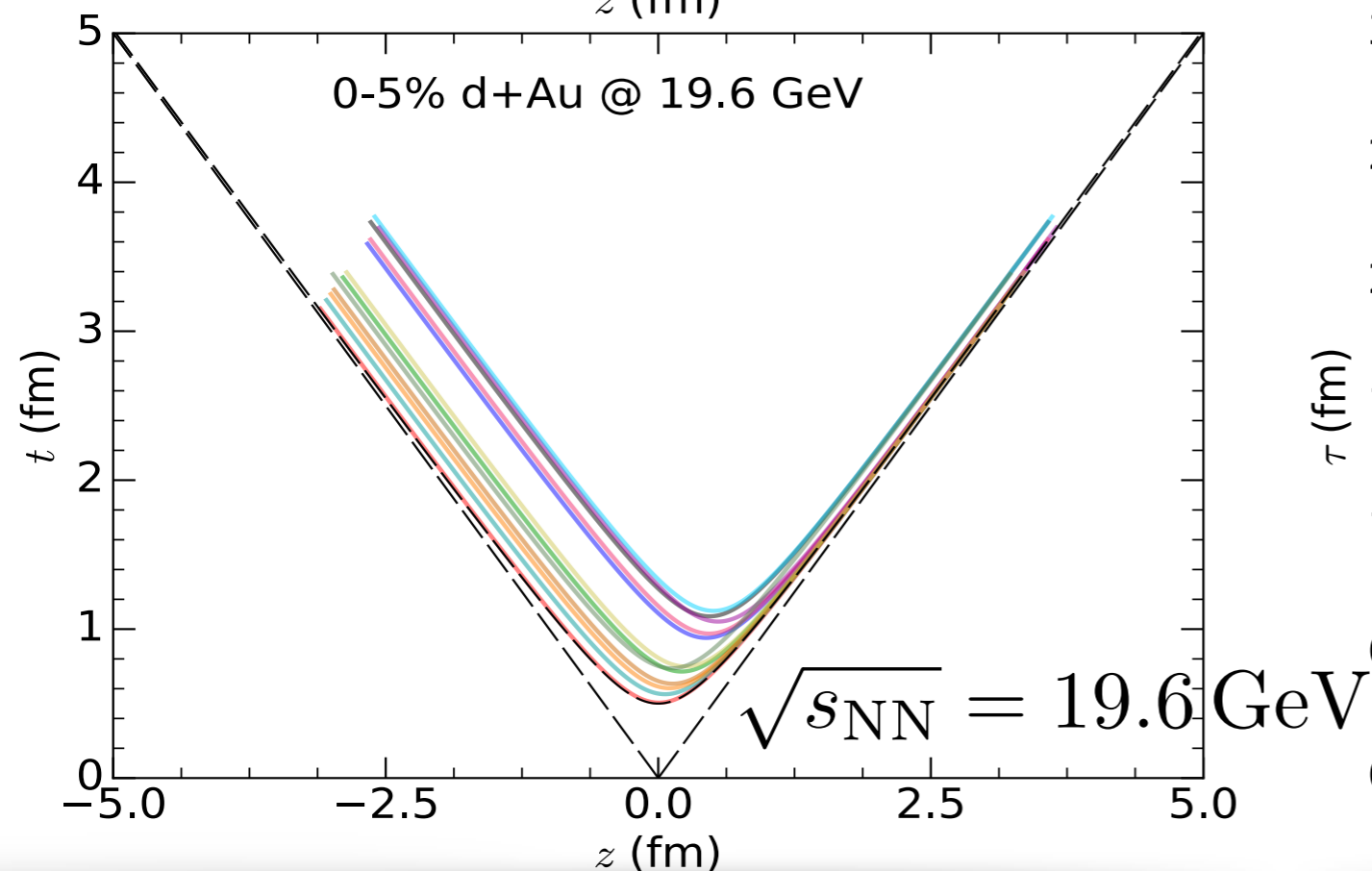
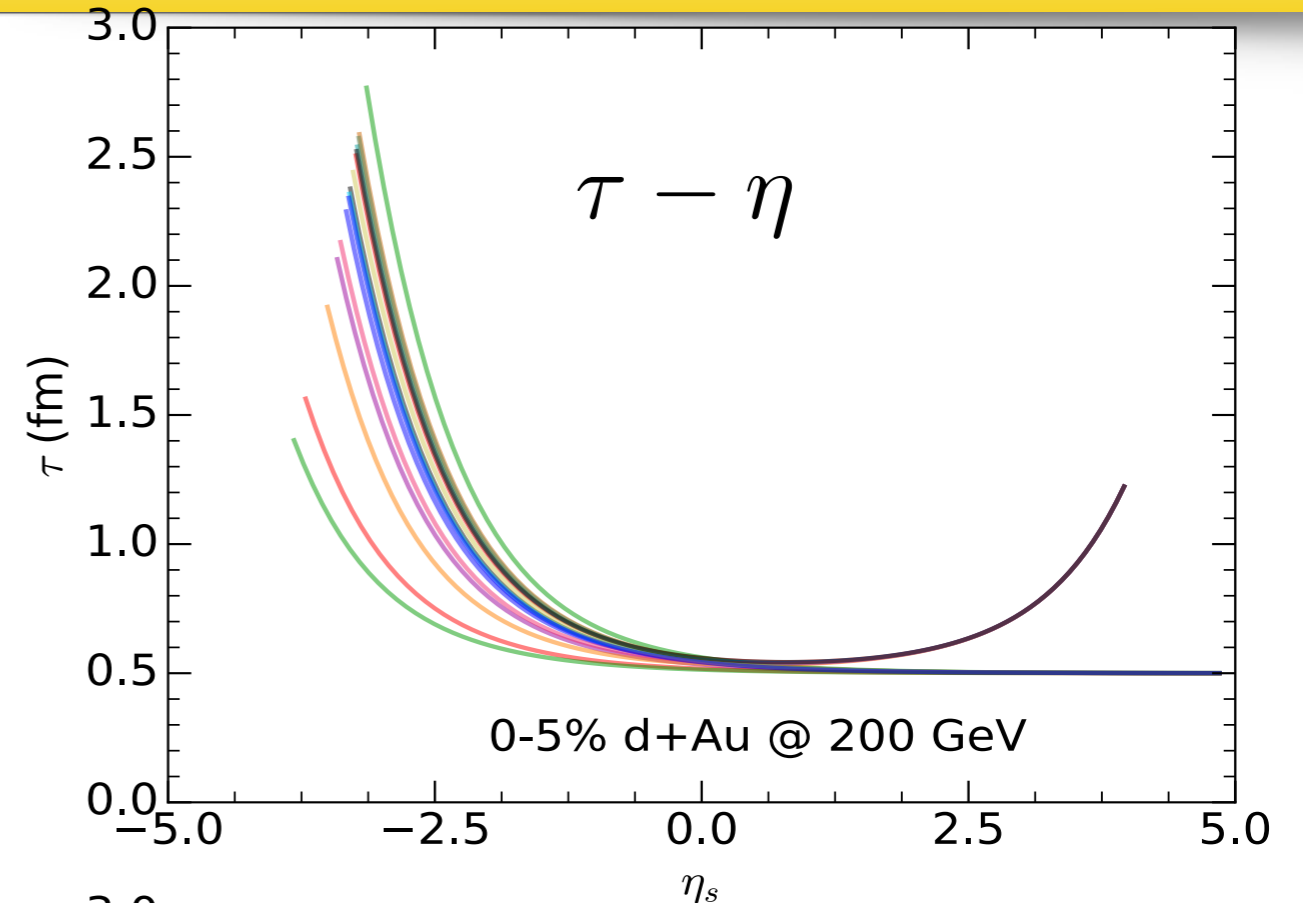
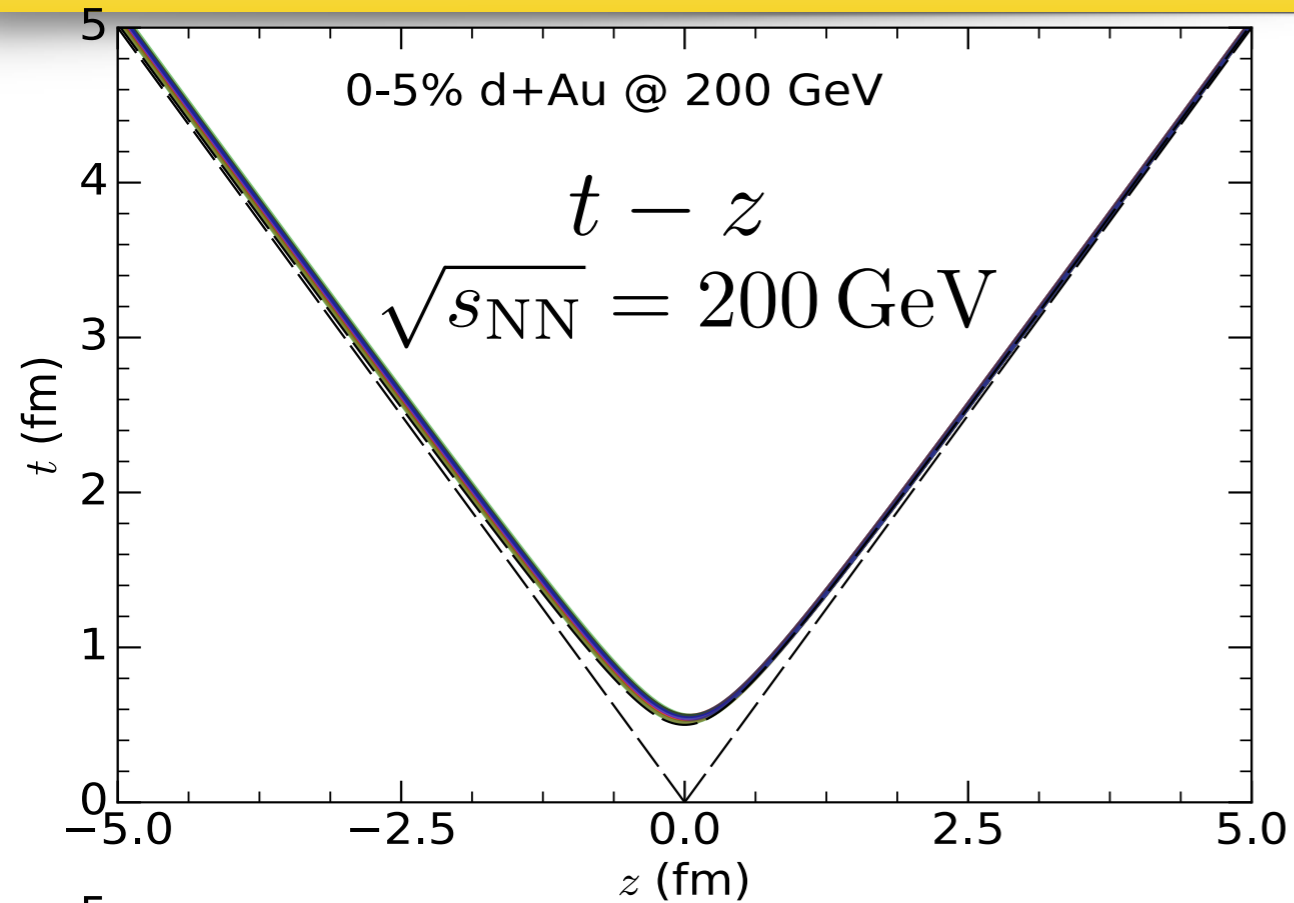
A 3D MCGlauber model



A 3D MCGlauber model



A 3D MCGlauber model

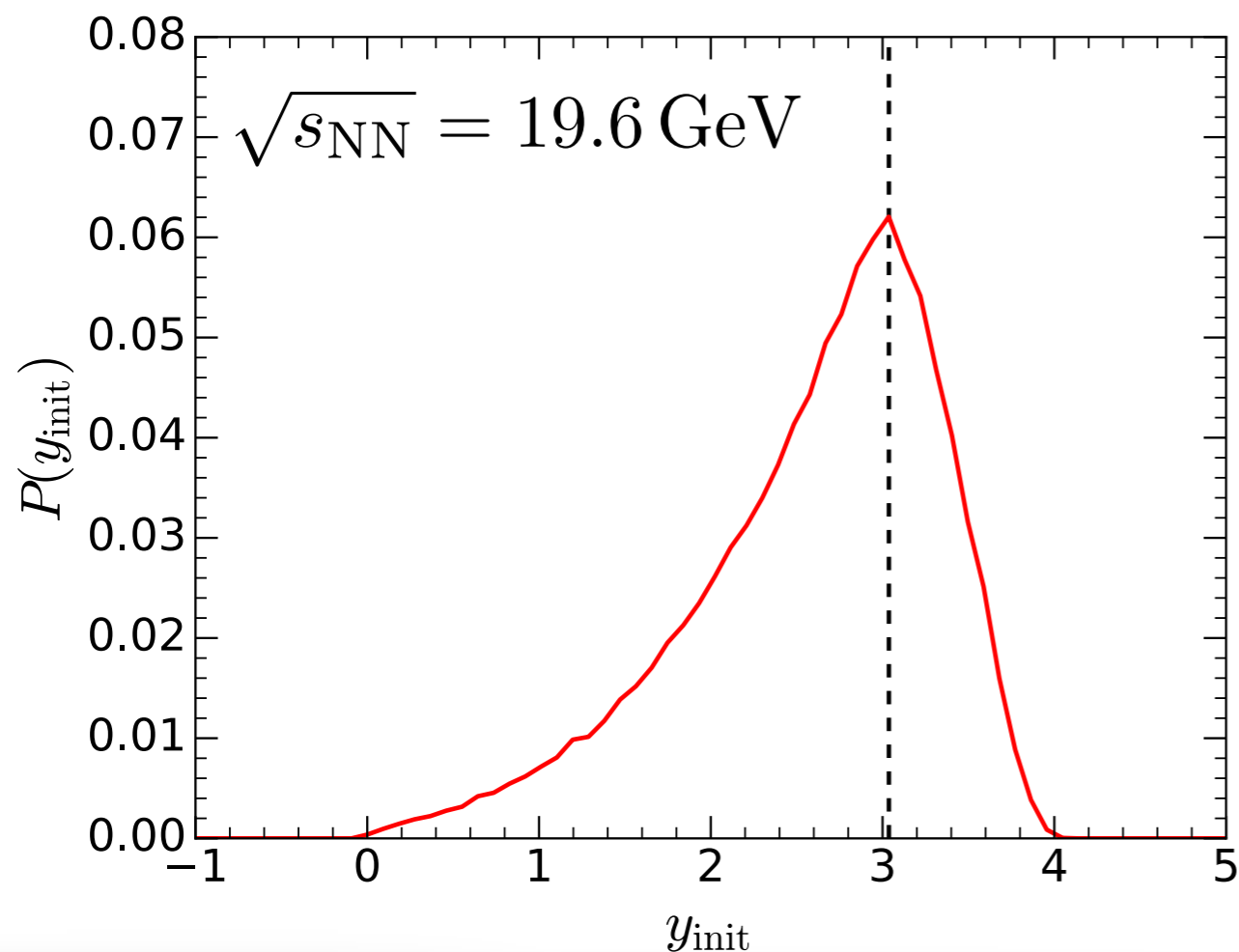


Introducing longitudinal fluctuations

- Sample valence quarks from the incoming participants

$$y_q = \operatorname{arcsinh} \left(x_q \sqrt{\frac{s}{4m_q^2} - 1} \right)$$

$$y_q = \log \left(\frac{x\sqrt{s}}{2m_q} \right)$$



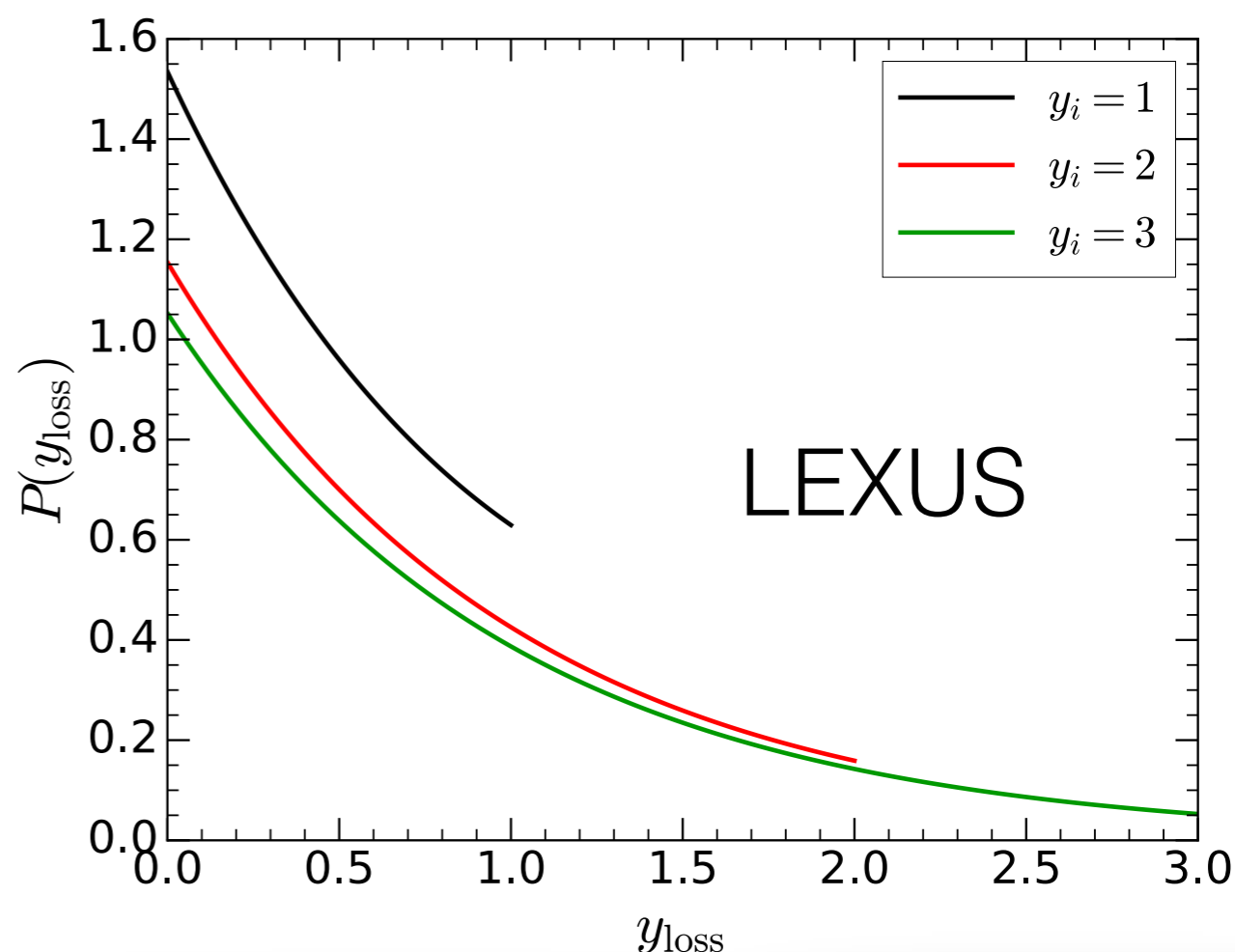
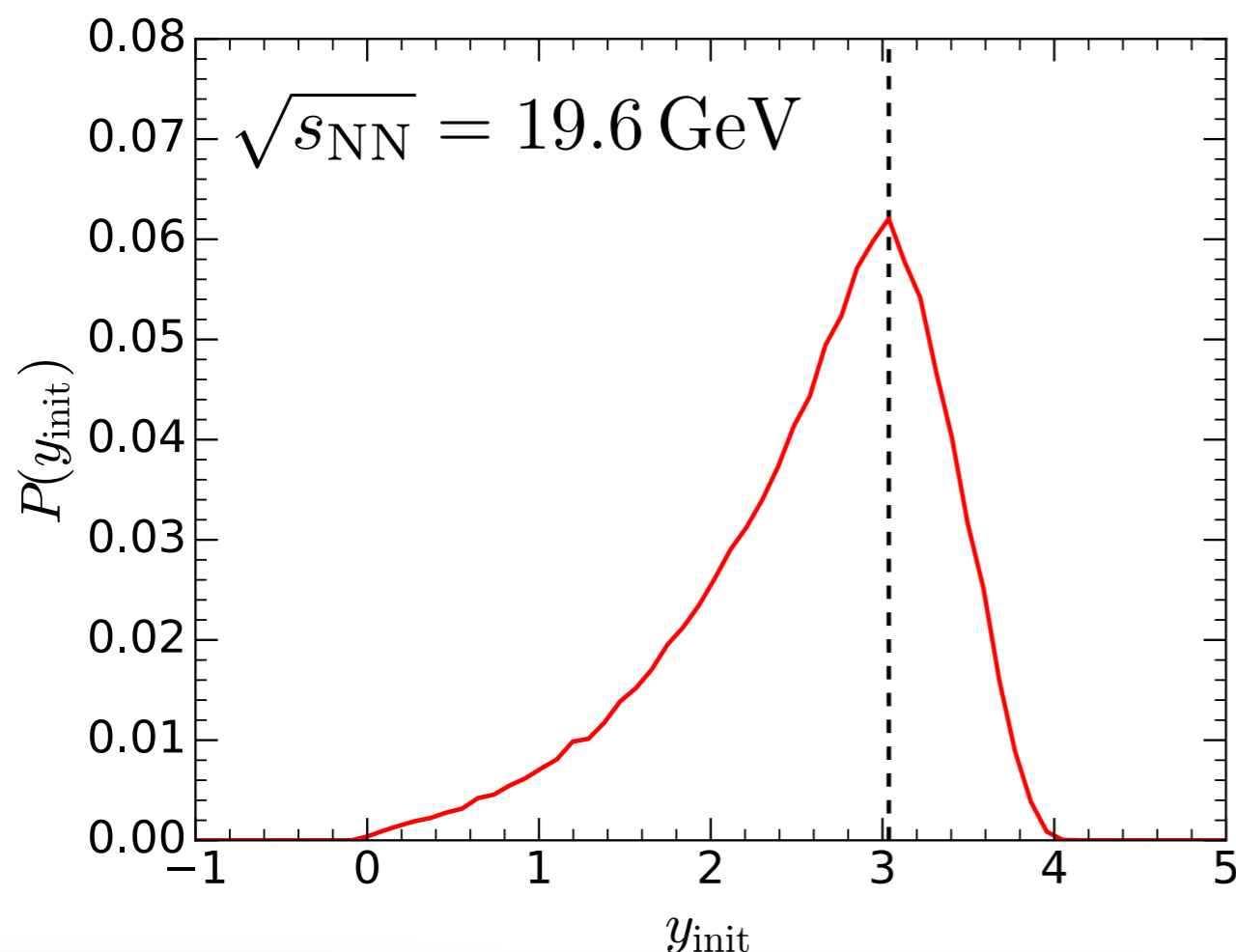
Introducing longitudinal fluctuations

- Sample valence quarks from the incoming participants

$$y_q = \operatorname{arcsinh} \left(x_q \sqrt{\frac{s}{4m_q^2} - 1} \right) \quad y_q = \log \left(\frac{x\sqrt{s}}{2m_q} \right)$$

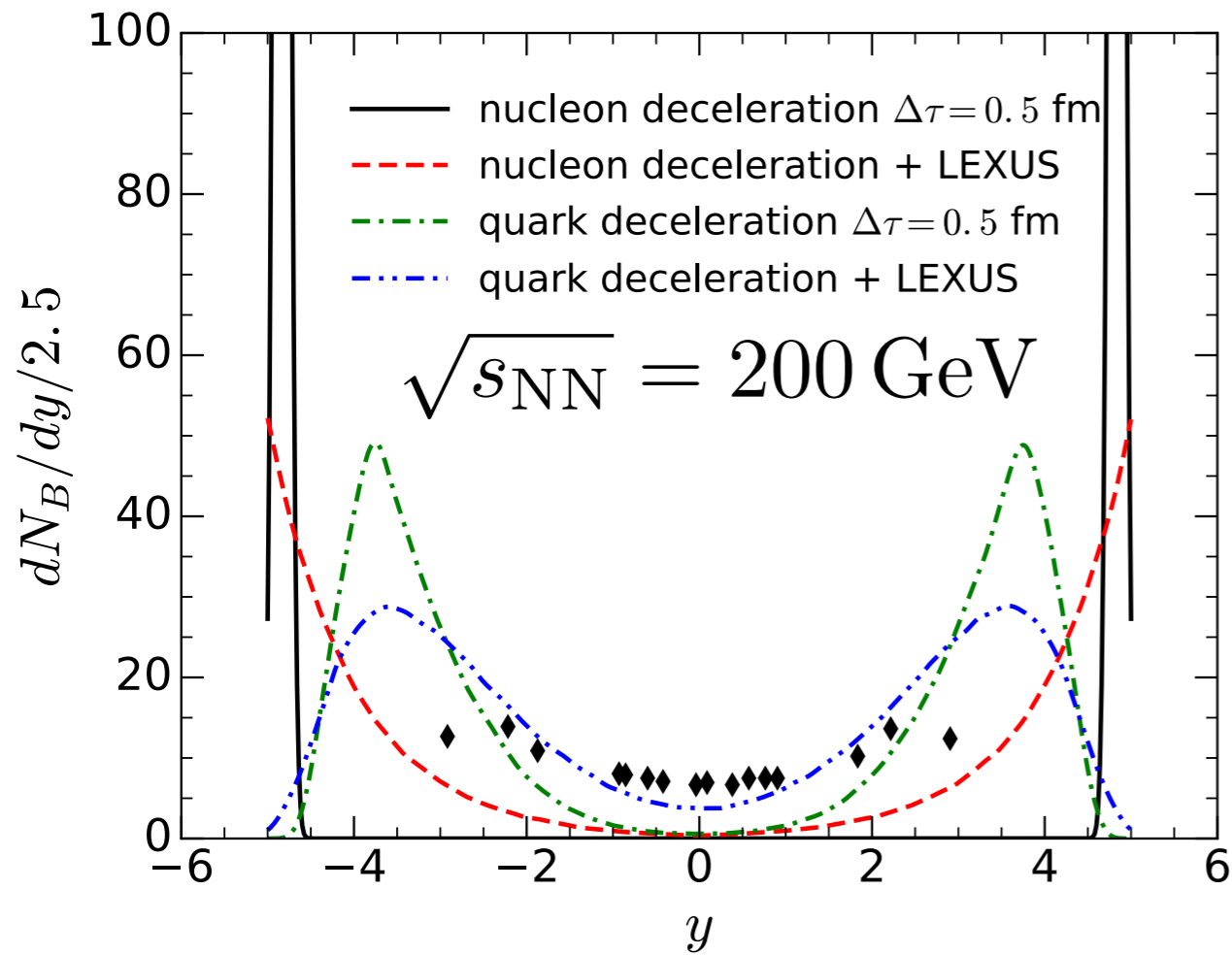
- Sample the rapidity loss according to the LEXUS model

$$P(y_{\text{loss}}) = \frac{\cosh(2y_{\text{init}} - y_{\text{loss}})}{\sinh(2y_{\text{init}}) - \sinh(y_{\text{init}})} \quad y_{\text{loss}} \in [0, y_{\text{init}}]$$



Net baryon rapidity distribution

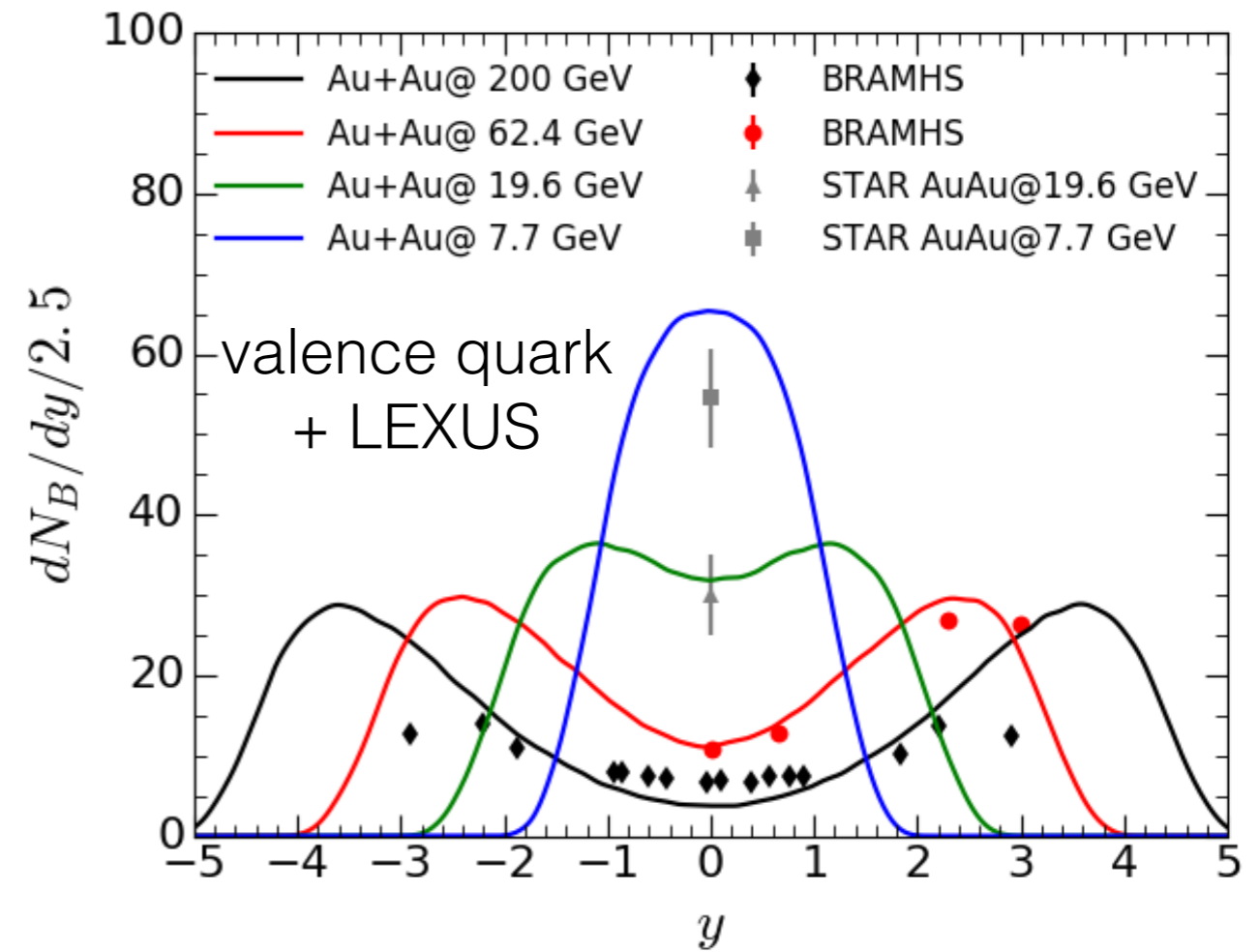
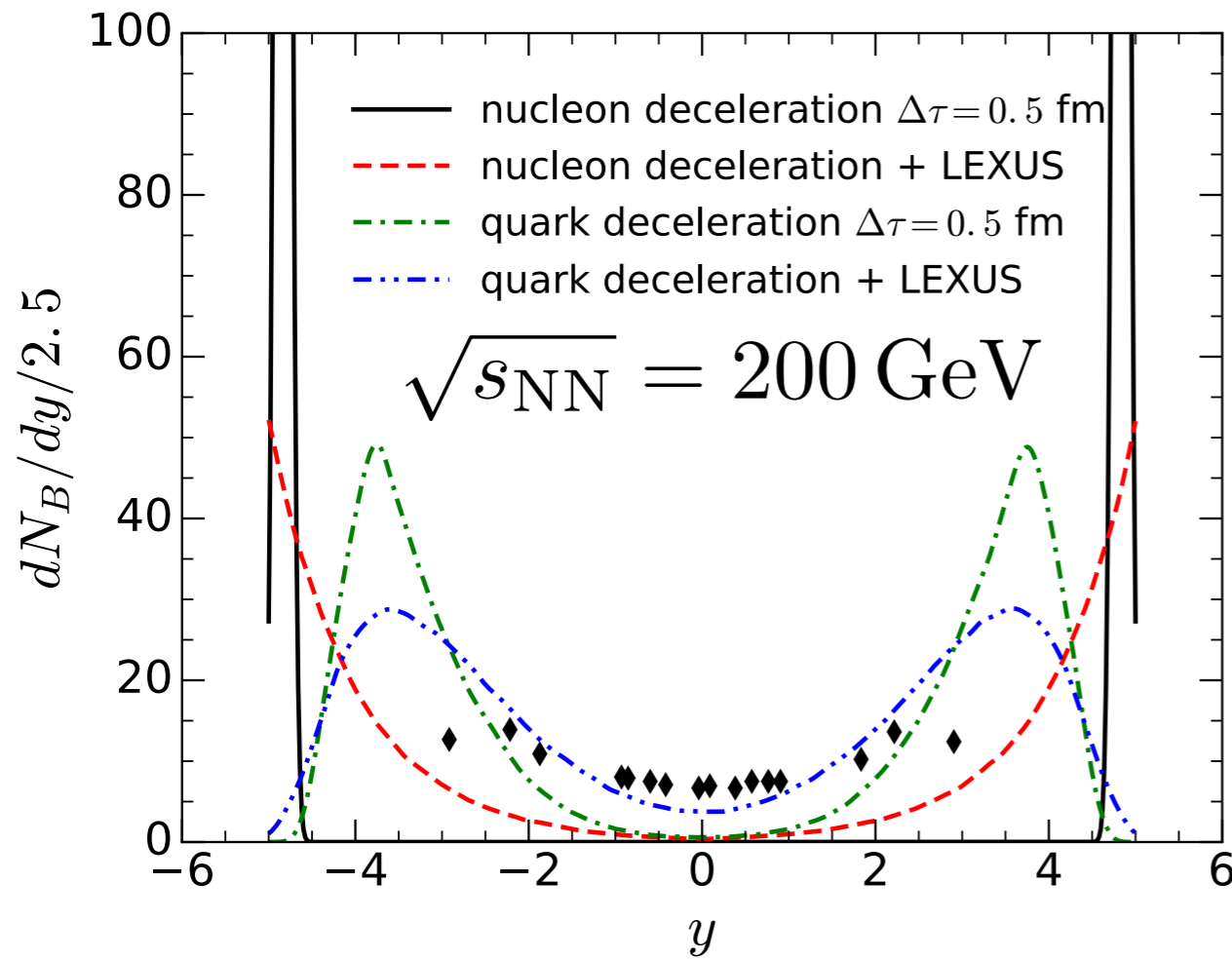
C. Shen, B. Schenke, in preparation



- Different rapidity fluctuation results different net baryon rapidity distribution

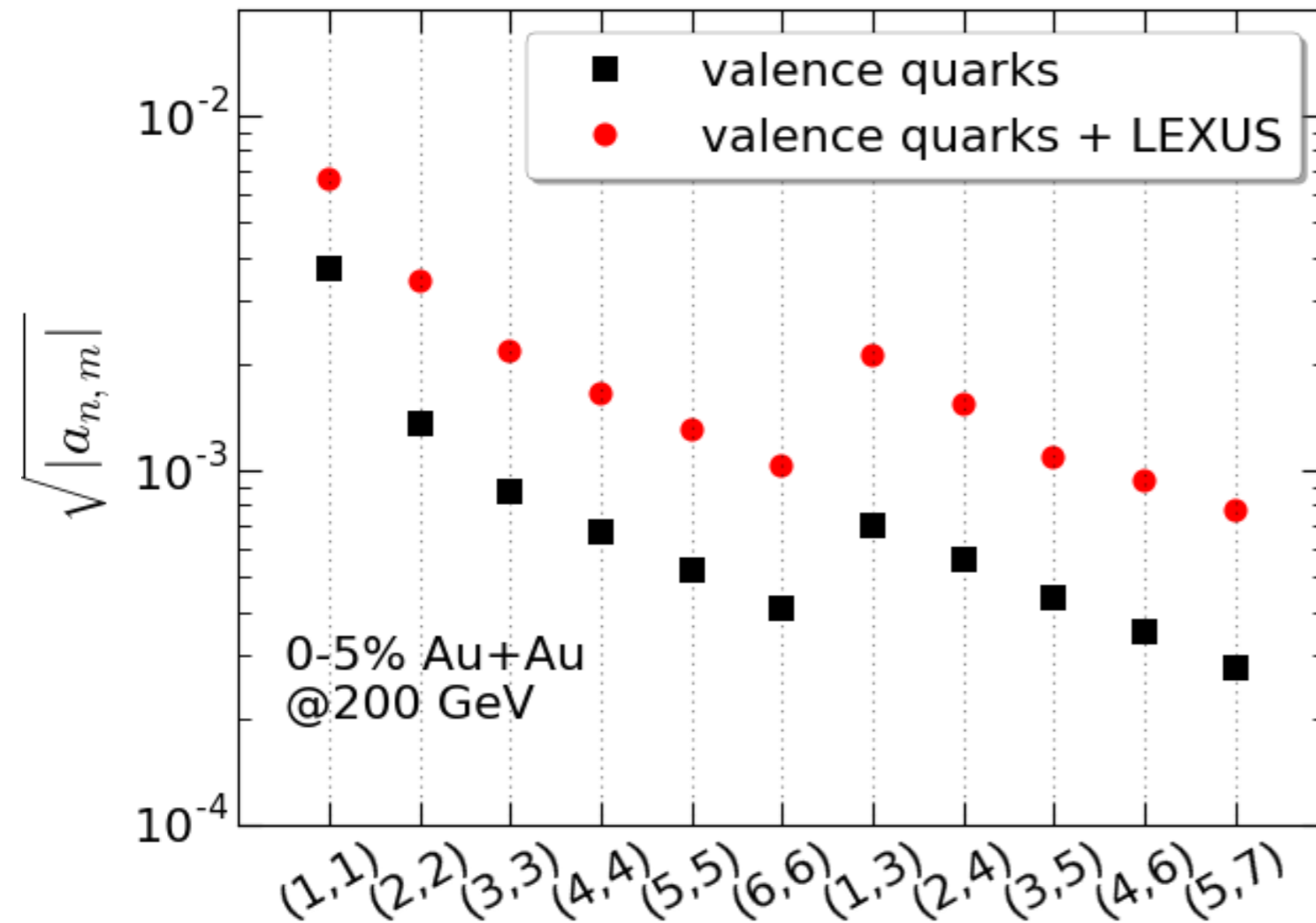
Net baryon rapidity distribution

C. Shen, B. Schenke, in preparation



- Different rapidity fluctuation results different net baryon rapidity distribution
- The valence quark + LEXUS model provides a reasonable net baryon rapidity distribution compared to the RHIC BES data

Quantify rapidity fluctuation



$$C(\eta_1, \eta_2) = \frac{\langle \frac{dN}{d\eta}(\eta_1) \frac{dN}{d\eta}(\eta_2) \rangle}{\langle \frac{dN}{d\eta}(\eta_1) \rangle \langle \frac{dN}{d\eta}(\eta_2) \rangle},$$

$$C_N(\eta_1, \eta_2) = \frac{C(\eta_1, \eta_2)}{C_p(\eta_1)C_p(\eta_2)},$$

$$C_p(\eta) = \frac{1}{2Y} \int_{-Y}^Y C(\eta_1, \eta_2) d\eta_2$$

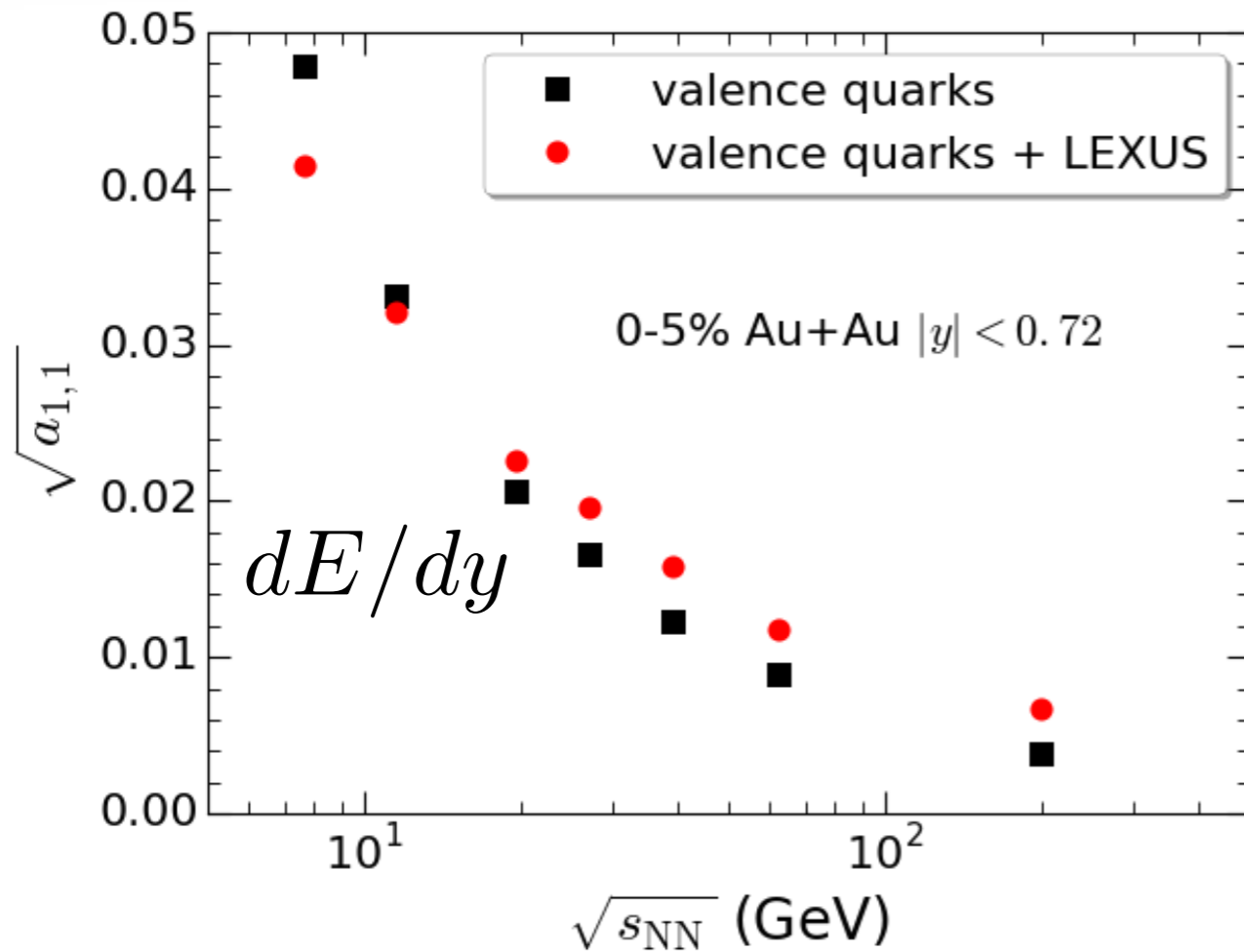
$$a_{n,m} = \int \frac{d\eta_1}{Y} \frac{d\eta_2}{Y} C_N(\eta_1, \eta_2) \frac{T_n(\eta_1)T_m(\eta_2) + T_n(\eta_2)T_m(\eta_1)}{2}$$

$$T_n(\eta) = \sqrt{n + \frac{1}{2}P_n\left(\frac{\eta}{Y}\right)}$$

- The size of the $a_{n,m}$ coefficient can quantify the amount of longitudinal fluctuations

Quantify rapidity fluctuation

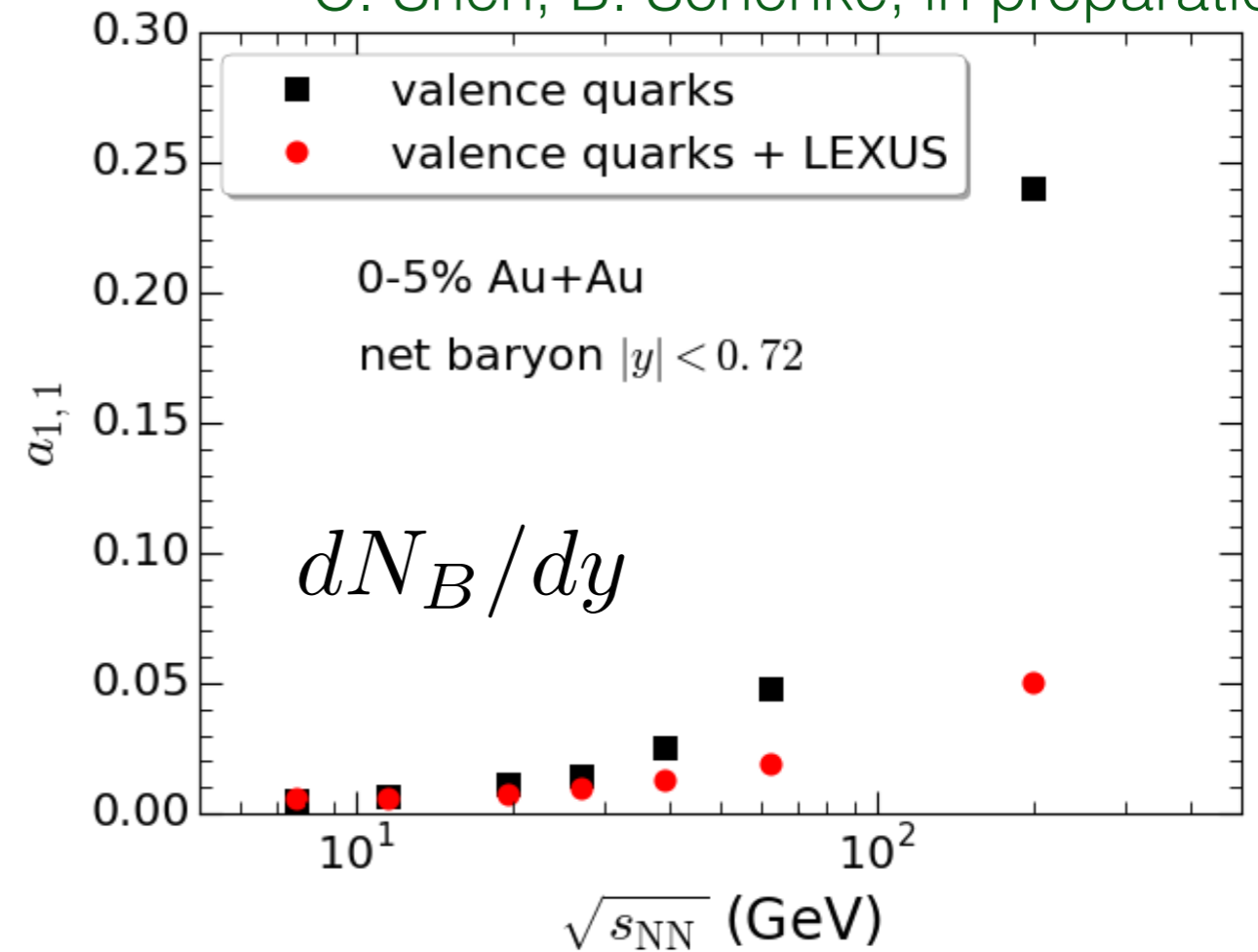
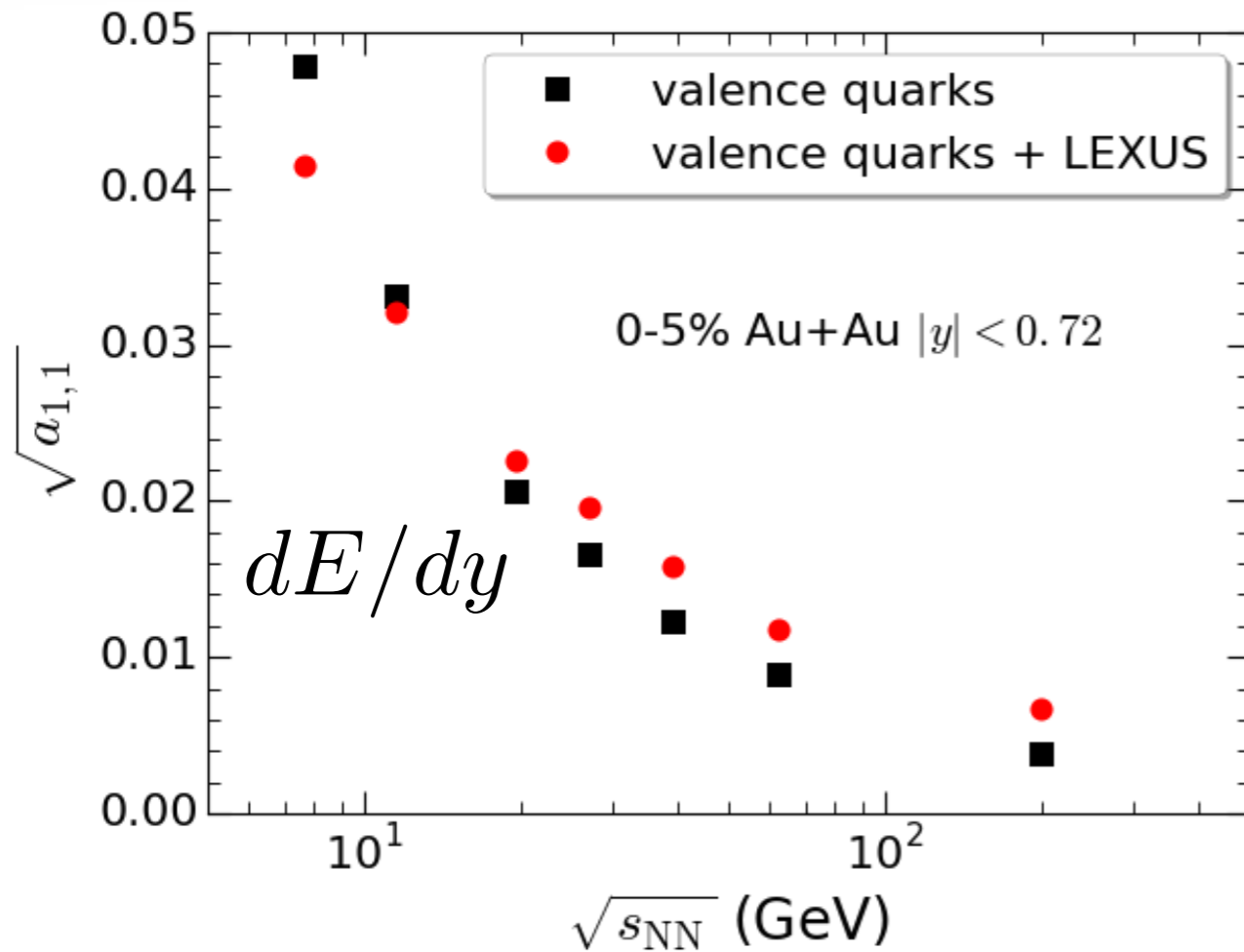
C. Shen, B. Schenke, in preparation



- The a_{11} coefficient for dE/dy decreases at high collision energy because the system becomes more boost-invariant

Quantify rapidity fluctuation

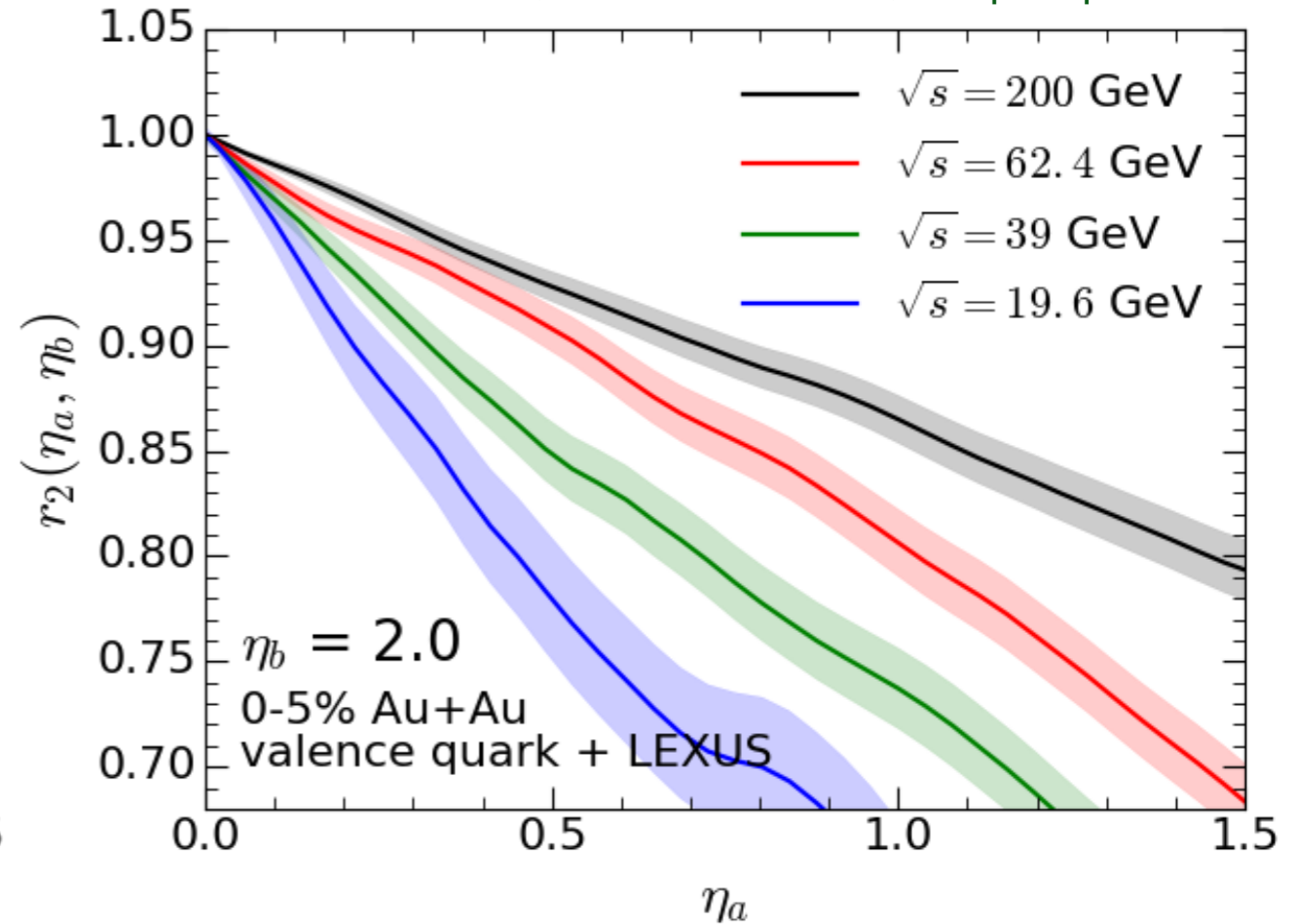
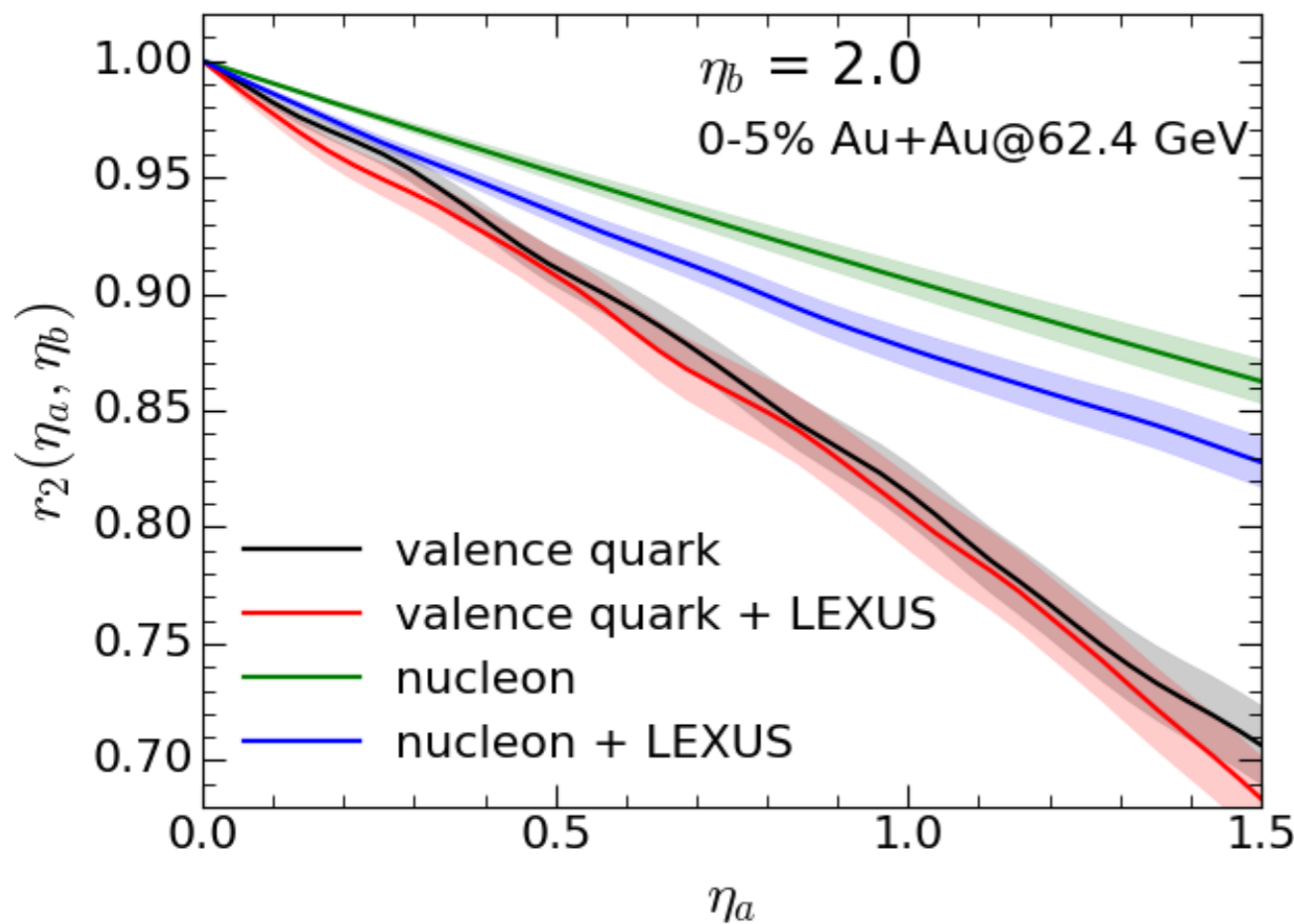
C. Shen, B. Schenke, in preparation



- The a_{11} coefficient for dE/dy decreases at high collision energy because the system becomes more boost-invariant
- The a_{11} coefficient for dN_B/dy increases at high collision energy because less net baryon number at mid-rapidity

Quantify rapidity fluctuation

C. Shen, B. Schenke, in preparation



$$r_n(\eta_a, \eta_b) = \frac{\langle \Re \{ \mathcal{E}_n(-\eta_a) \cdot \mathcal{E}_n^*(\eta_b) \} \rangle_{ev}}{\langle \Re \{ \mathcal{E}_n(\eta_a) \cdot \mathcal{E}_n^*(\eta_b) \} \rangle_{ev}}$$

$$\mathcal{E}_n(\eta) = - \frac{\int r dr d\phi r^n e(r, \phi, \eta) e^{in\phi}}{\int r dr d\phi r^n e(r, \phi, \eta)}$$

- The initial eccentricities decorrelate along η direction faster with more longitudinal fluctuation and at lower collision energy

Hydrodynamics with sources

Energy-momentum current and net baryon density are feed into hydrodynamic simulation as source terms

$$\partial_\mu T^{\mu\nu} = J_{\text{source}}^\nu$$

$$\partial_\mu J^\mu = \rho_{\text{source}}$$

where

$$J_{\text{source}}^\nu = \delta e u^\nu + (e + P) \delta u^\nu$$

$$\delta u^\nu = \frac{\Delta_{\mu}^{\nu} J_{\text{source}}^{\mu}}{e + P}$$

δe heats up the system

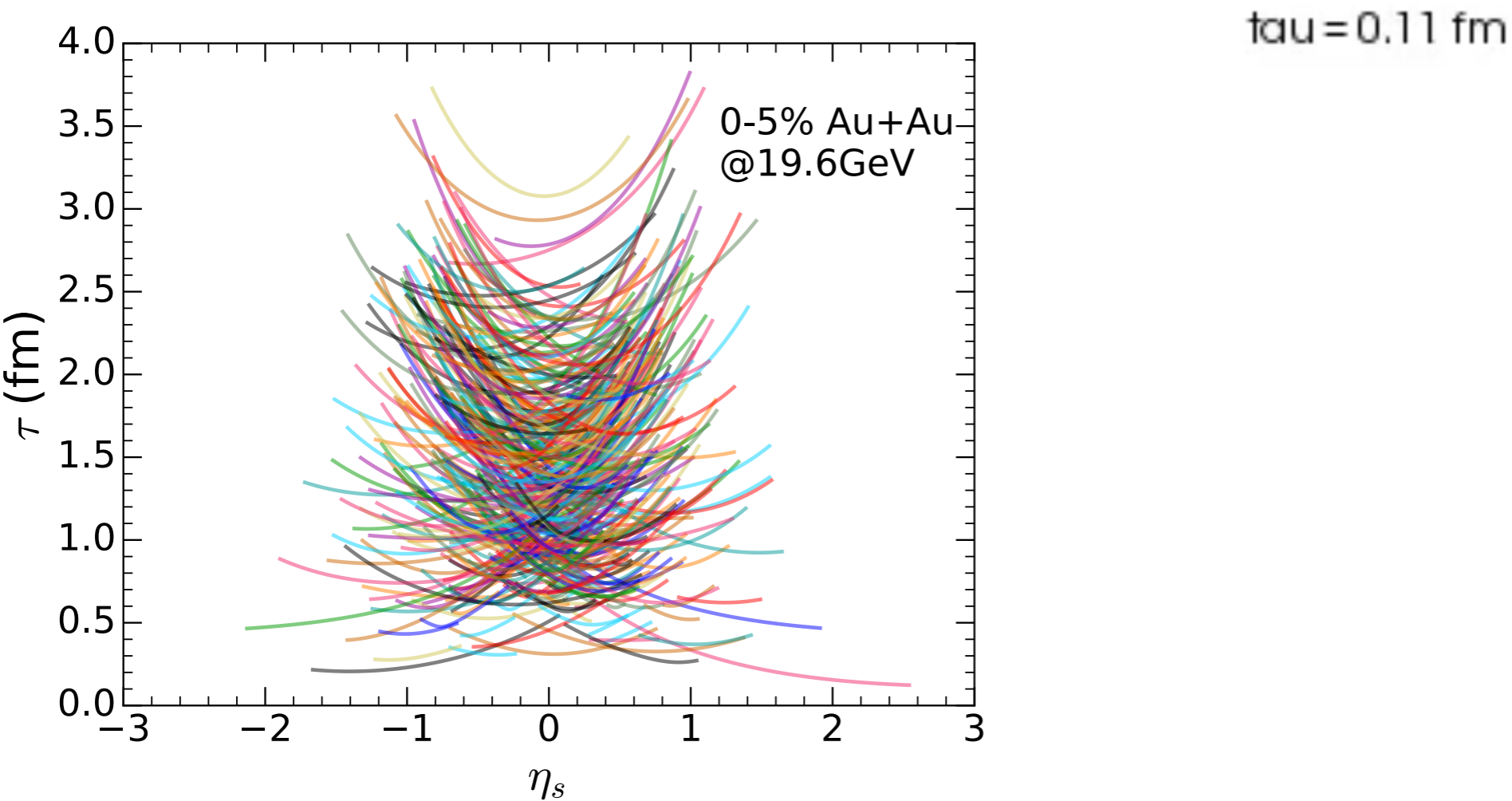
δu^ν accelerates the flow velocity

ρ_{source} dopes baryon charges into the system

- Source terms are smeared with Gaussians in space and time

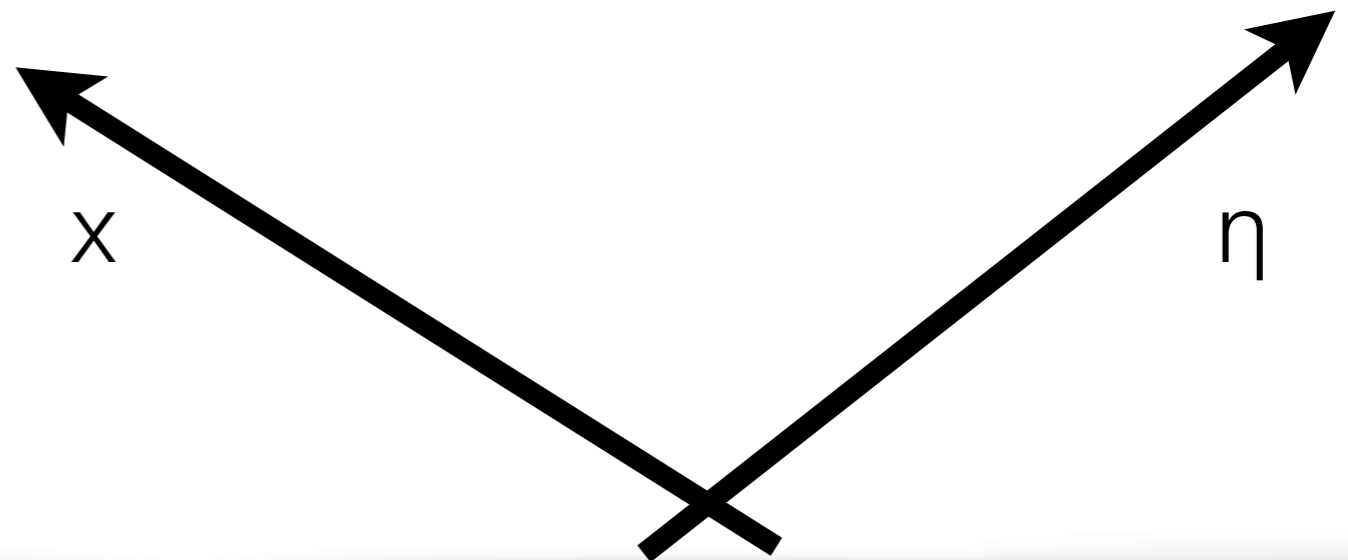
Hydrodynamical evolution with sources

energy density



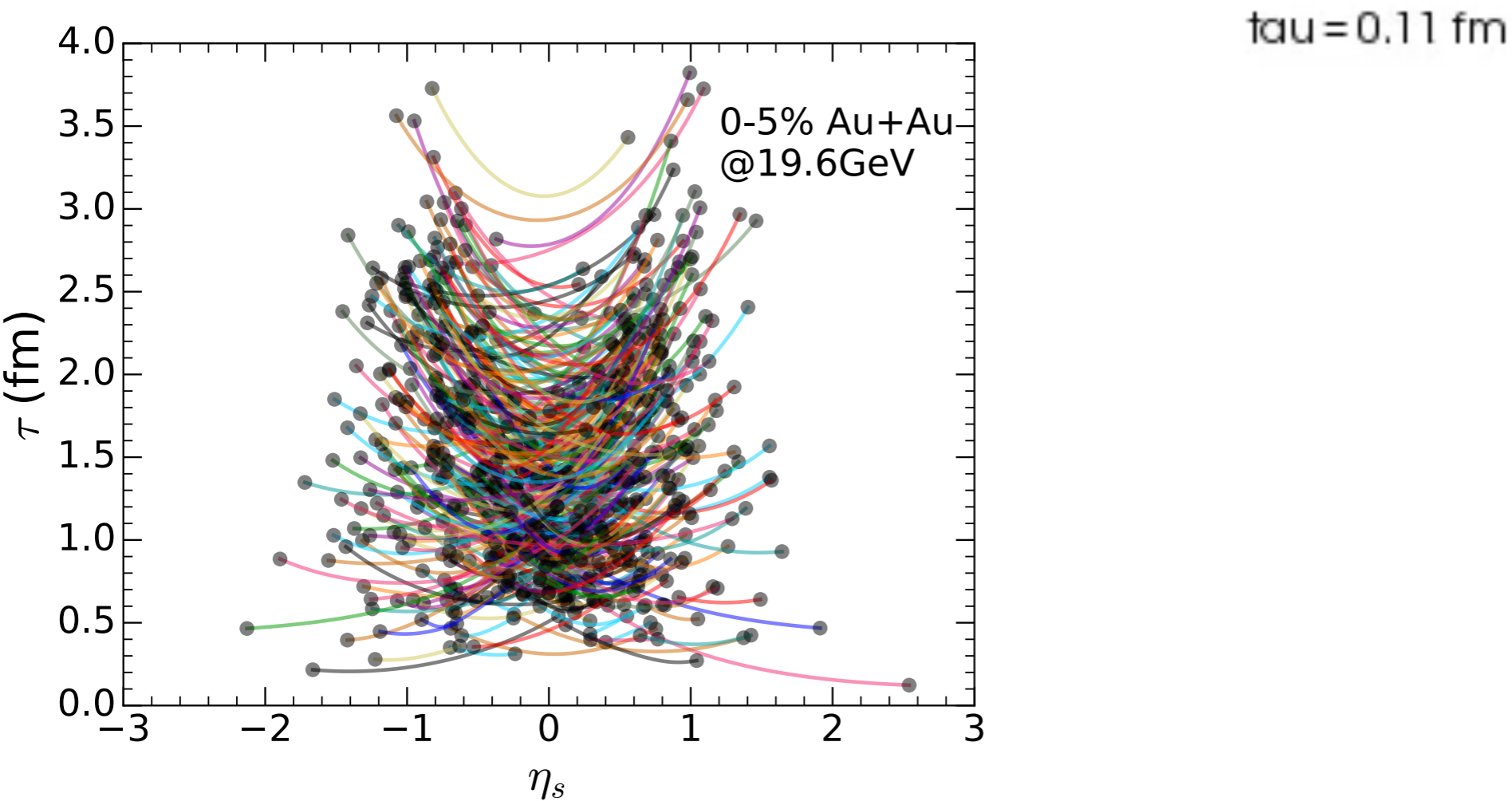
$$\sqrt{s_{NN}} = 19.6 \text{ GeV}$$

valence quark + LEXUS



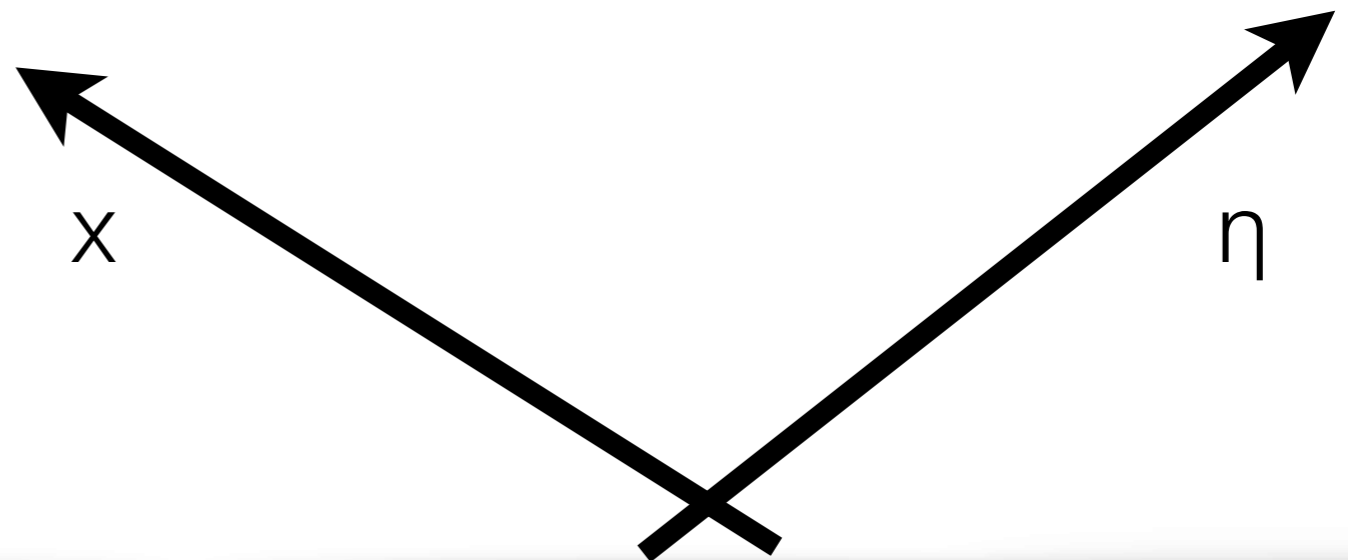
Hydrodynamical evolution with sources

net baryon density



$$\sqrt{s_{NN}} = 19.6 \text{ GeV}$$

valence quark + LEXUS



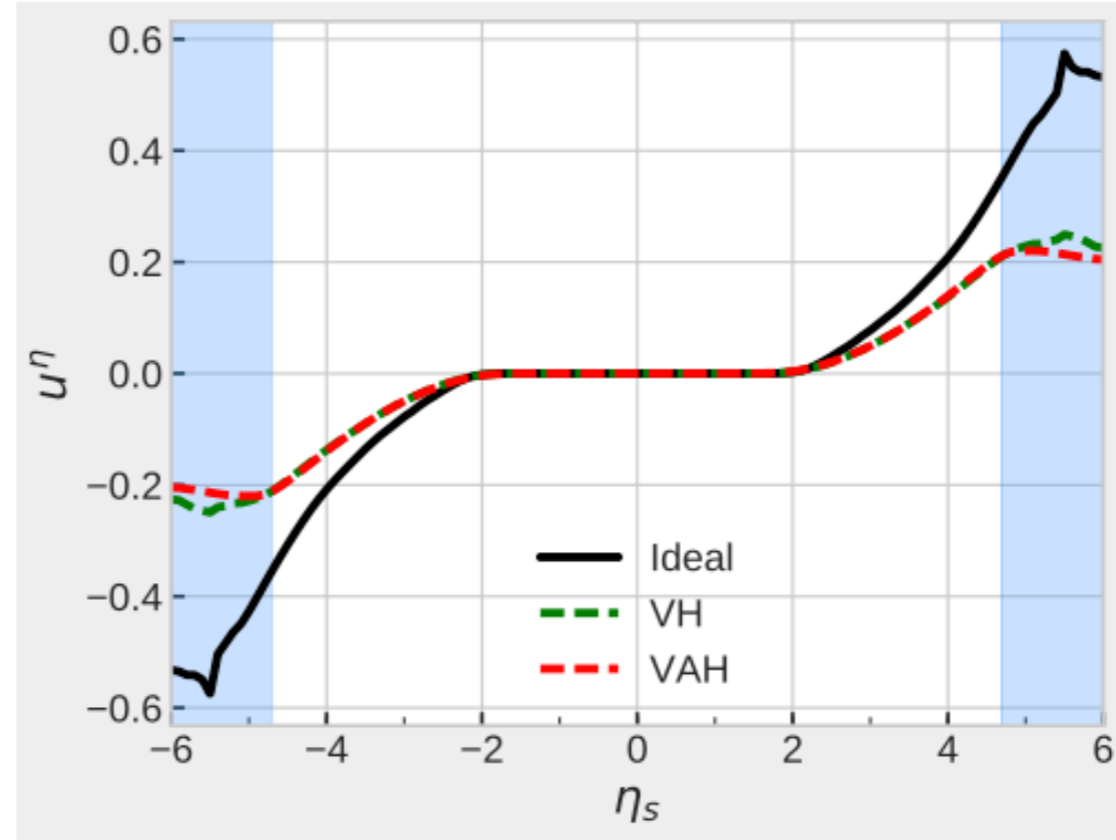
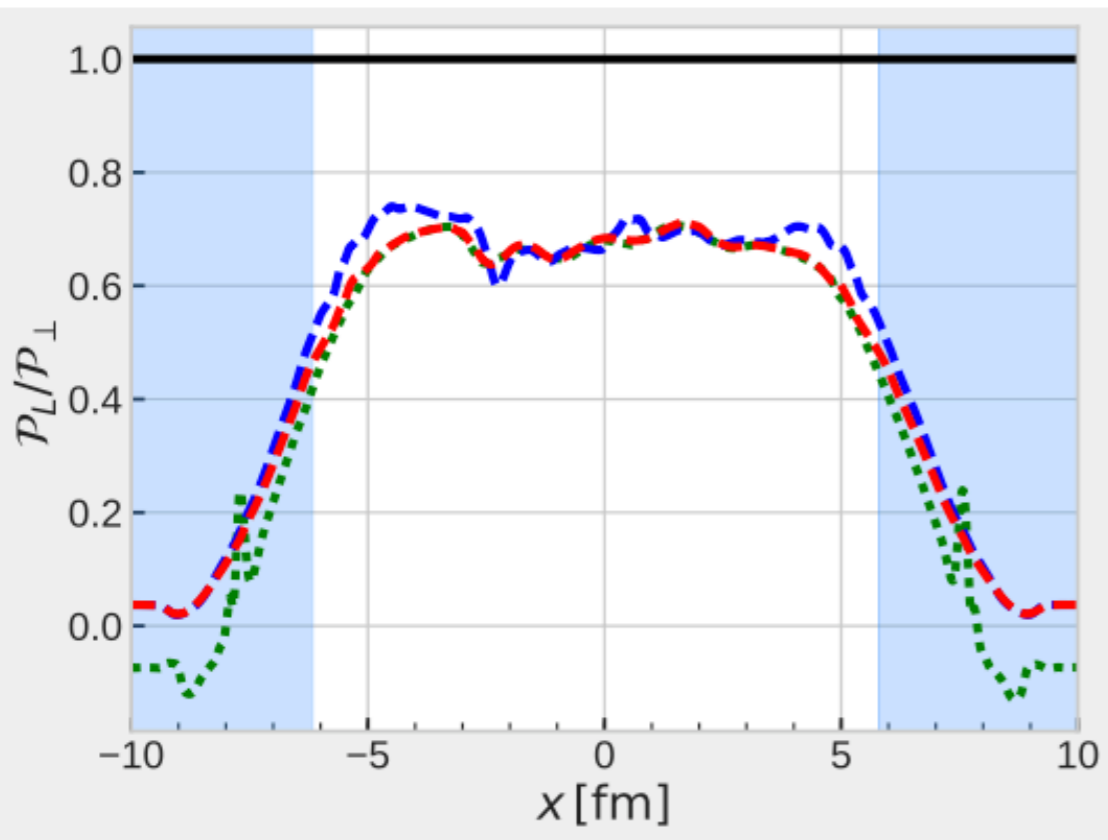
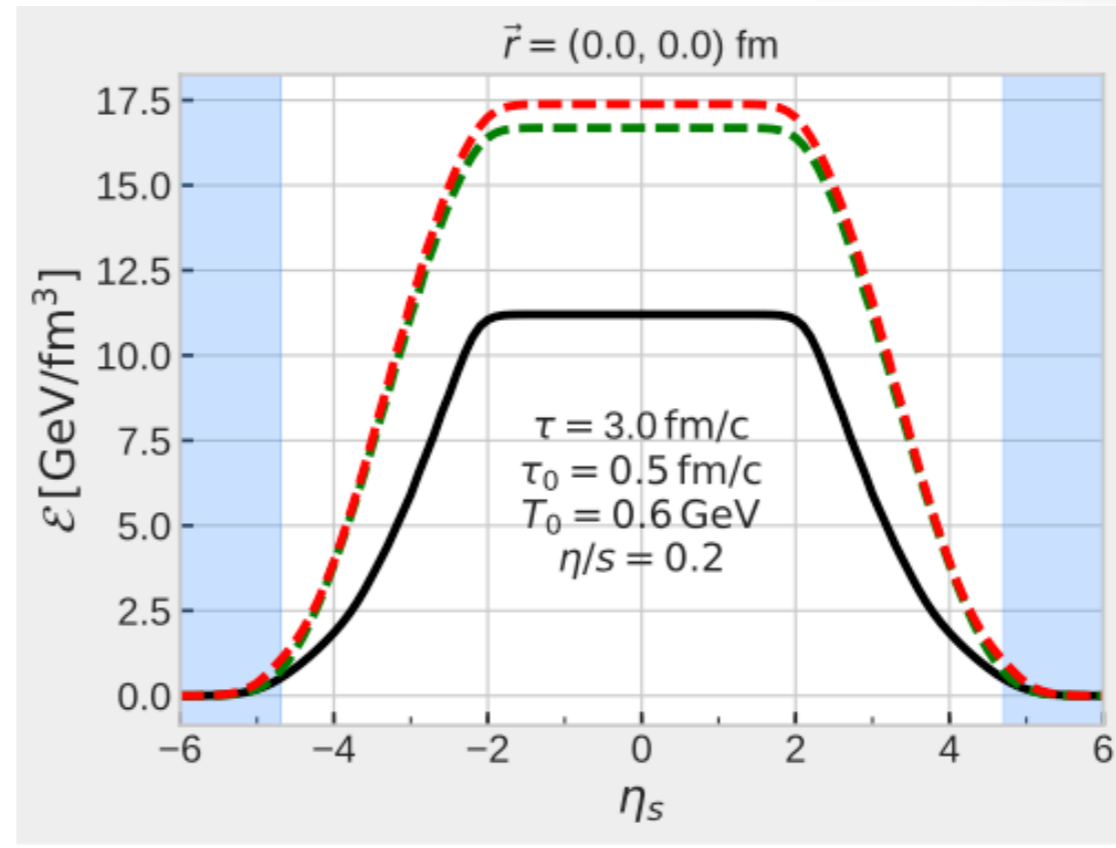
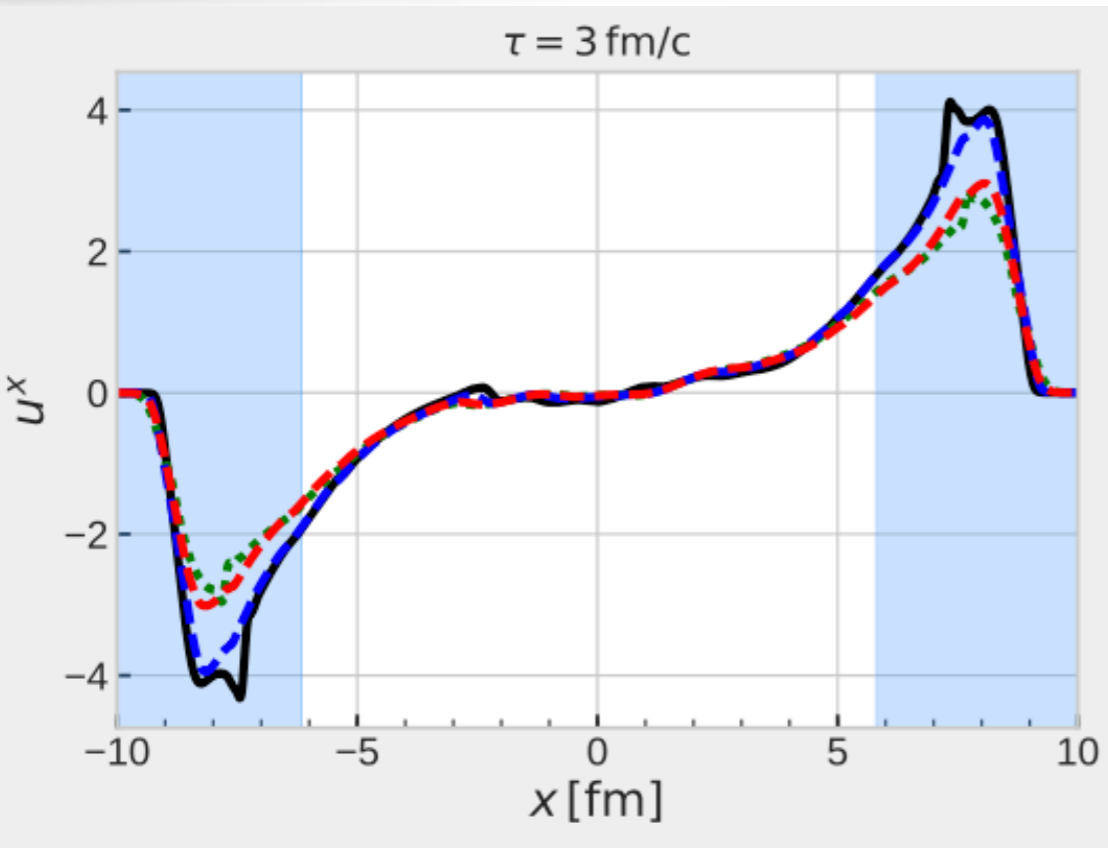


Progress in hydrodynamics

(3+1)D vHydro and vaHydro — a comparison



$\tau_0 = 0.5 \text{ fm/c}$
 $T_0 = 0.6 \text{ GeV}$
 $\eta/s = 0.2$



Dissipative hydrodynamics

Energy momentum tensor

$$T^{\mu\nu} = e u^\mu u^\nu - (P + \Pi) \Delta^{\mu\nu} + \pi^{\mu\nu} \quad \Delta^{\mu\nu} = g^{\mu\nu} - u^\mu u^\nu$$

Conserved currents

$$J^\mu = n u^\mu + q^\mu$$

Equations of motion

$$\begin{aligned} \partial_\mu T^{\mu\nu} &= 0 \\ \partial_\mu J^\mu &= 0 \end{aligned} \quad + \quad P(e, n)$$

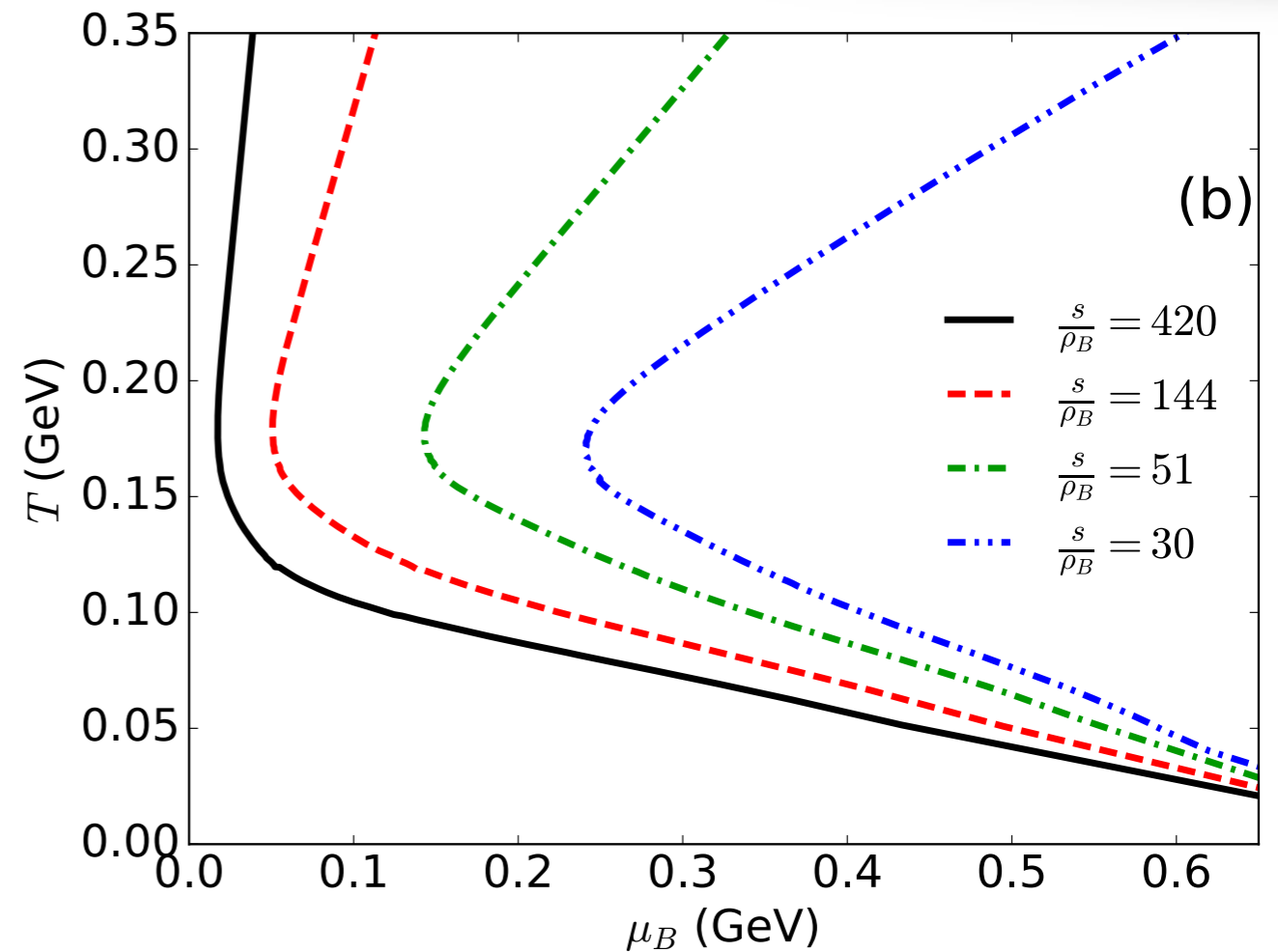
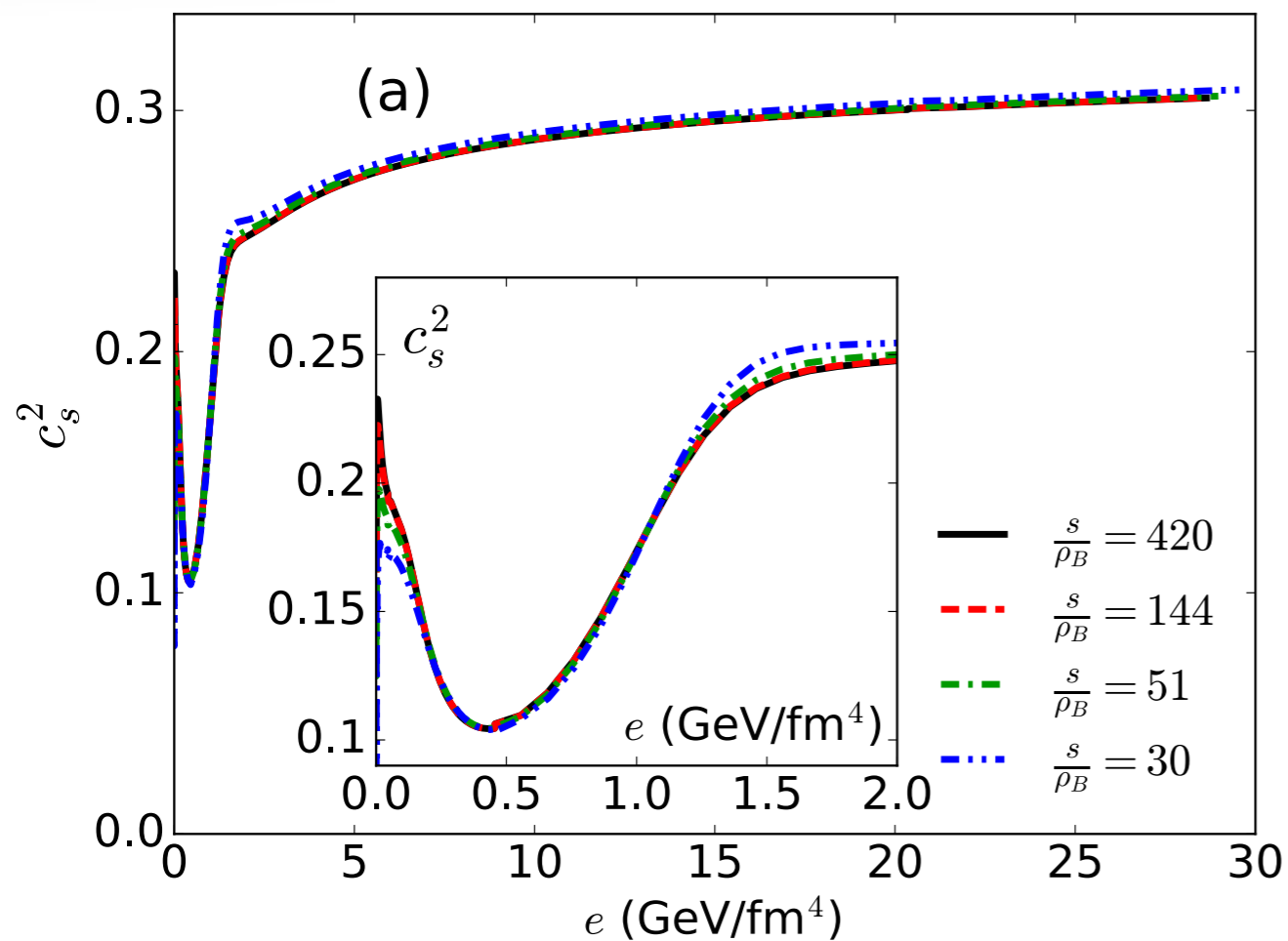
Dissipative quantities are evolved with 2nd order Israel-Stewart type of equations

At Navier-Stokes limit,

$$\pi^{\mu\nu} \sim 2\eta \nabla^{\langle\mu} u^{\nu\rangle} \quad \Pi \sim -\zeta \partial_\mu u^\mu \quad q^\mu \sim \kappa \nabla^\mu \frac{\mu}{T}$$

$$\nabla^\mu = \Delta^{\mu\nu} \partial_\nu$$

EoS at finite μ_B



High temperature:

- Lattice QCD EoS up to $\mathcal{O}(\mu_B^4)$

Low temperature:

- Glued with hadron resonance gas EoS

Transport coefficients

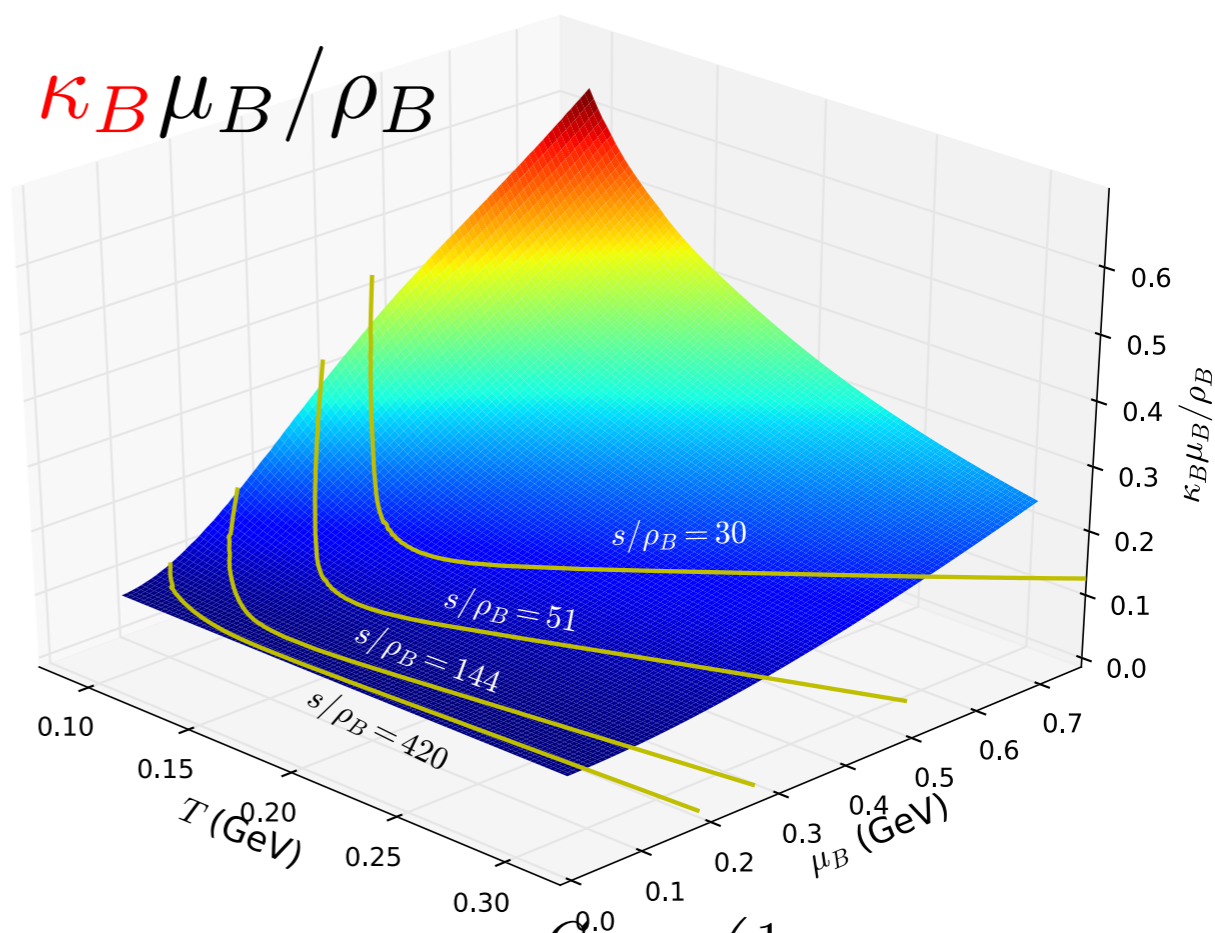
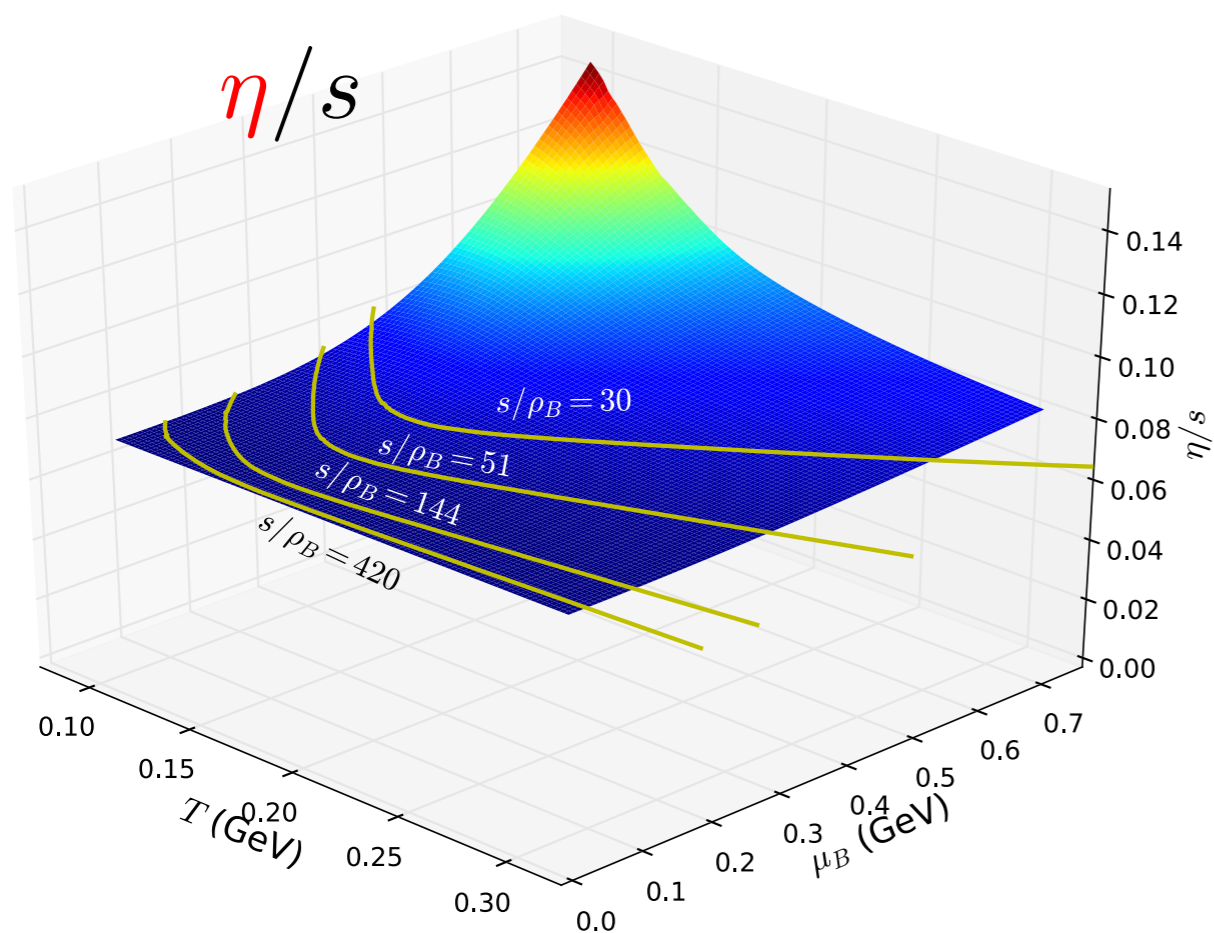
Dissipative part:

(relaxation time approximation)

$$\Delta_{\alpha\beta}^{\mu\nu} D\pi^{\alpha\beta} = -\frac{1}{\tau_\pi} (\pi^{\mu\nu} - 2\eta\sigma^{\mu\nu}) - \frac{\delta_{\pi\pi}}{\tau_\pi} \pi^{\mu\nu} \theta - \frac{\tau_{\pi\pi}}{\tau_\pi} \pi^\lambda \langle \mu \sigma^\nu \rangle_\lambda + \frac{\phi_7}{\tau_\pi} \pi_\alpha \langle \mu \pi^\nu \rangle_\alpha$$

$$\Delta^{\mu\nu} Dq_\nu = -\frac{1}{\tau_q} (q^\mu - \kappa \nabla^\mu \frac{\mu_B}{T}) - \frac{\delta_{qq}}{\tau_q} q^\mu \theta - \frac{\lambda_{qq}}{\tau_q} q_\nu \sigma^{\mu\nu}$$

With non-zero μ , we choose $\tau_\pi = \tau_q = \frac{0.4}{T} \quad \frac{\eta T}{e + \mathcal{P}} = 0.08$



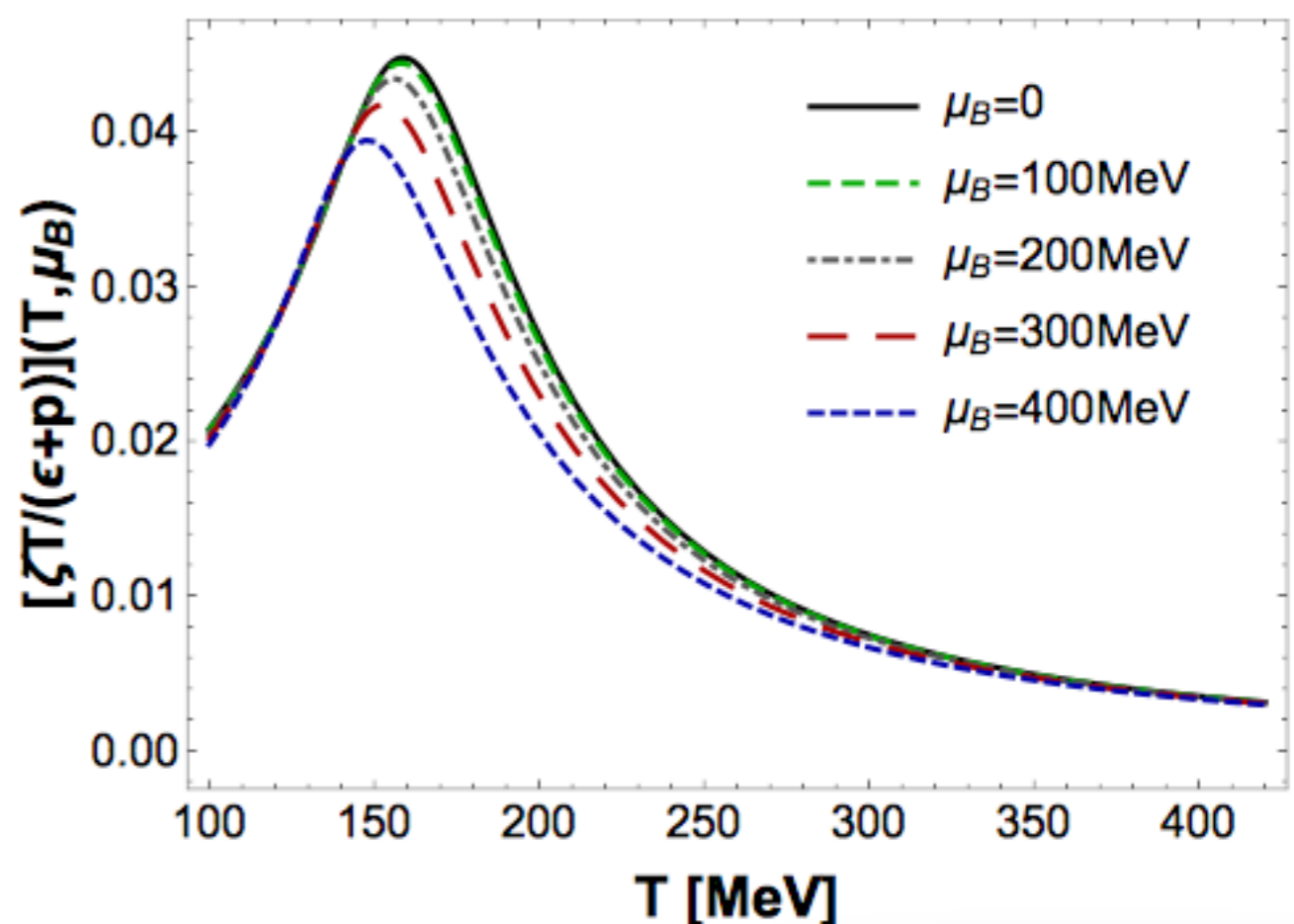
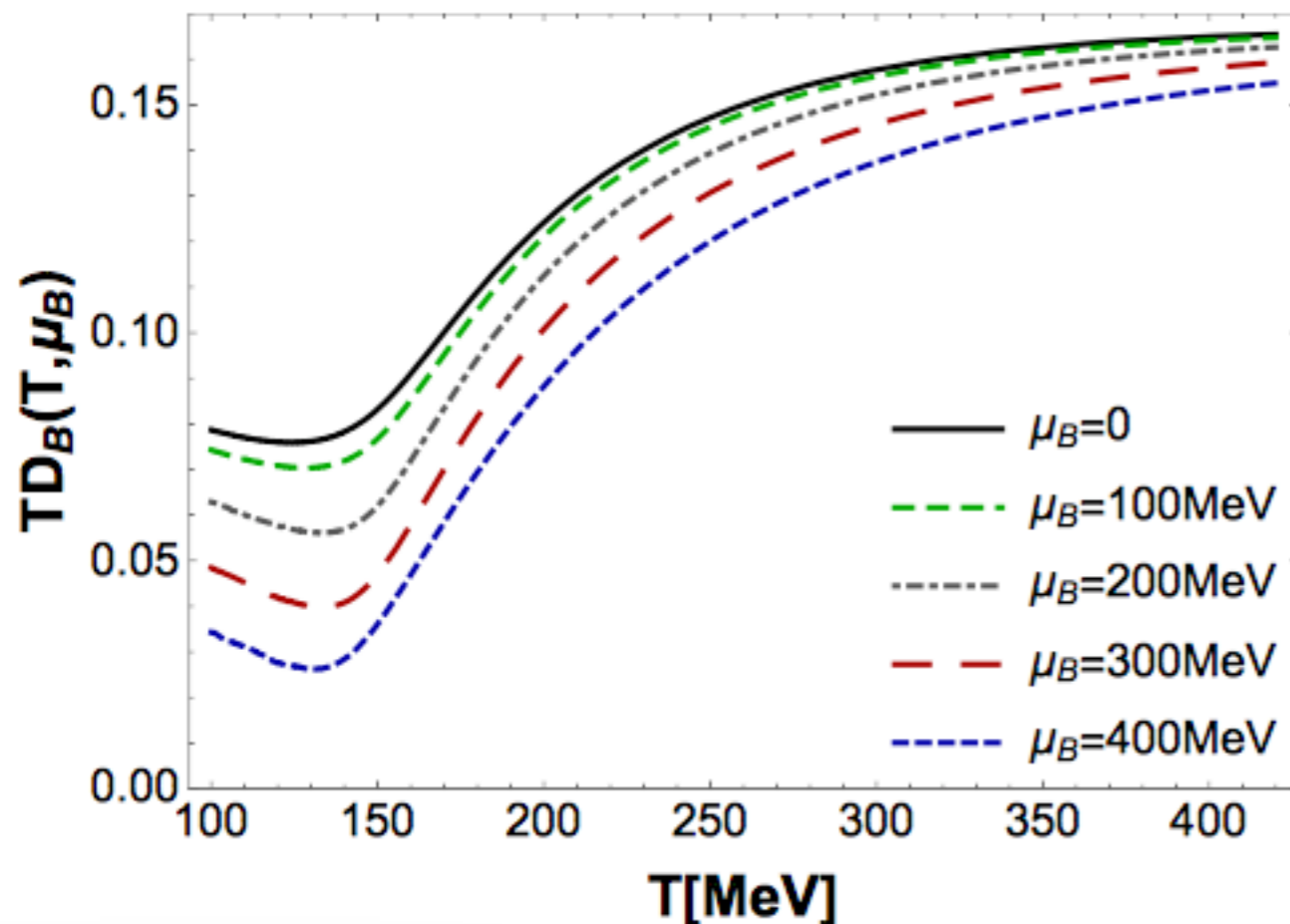
$$\kappa_B = \frac{C_B^{0,0}}{T} \rho_B \left(\frac{1}{3} \coth \left(\frac{\mu_B}{T} \right) - \frac{\rho_B T}{e + P} \right)$$

Transport coefficients

R. Rougemont, R. Critelli, J. Noronha-Hostler, J. Noronha and C. Ratti, Phys. Rev. D 96, 014032 (2017)

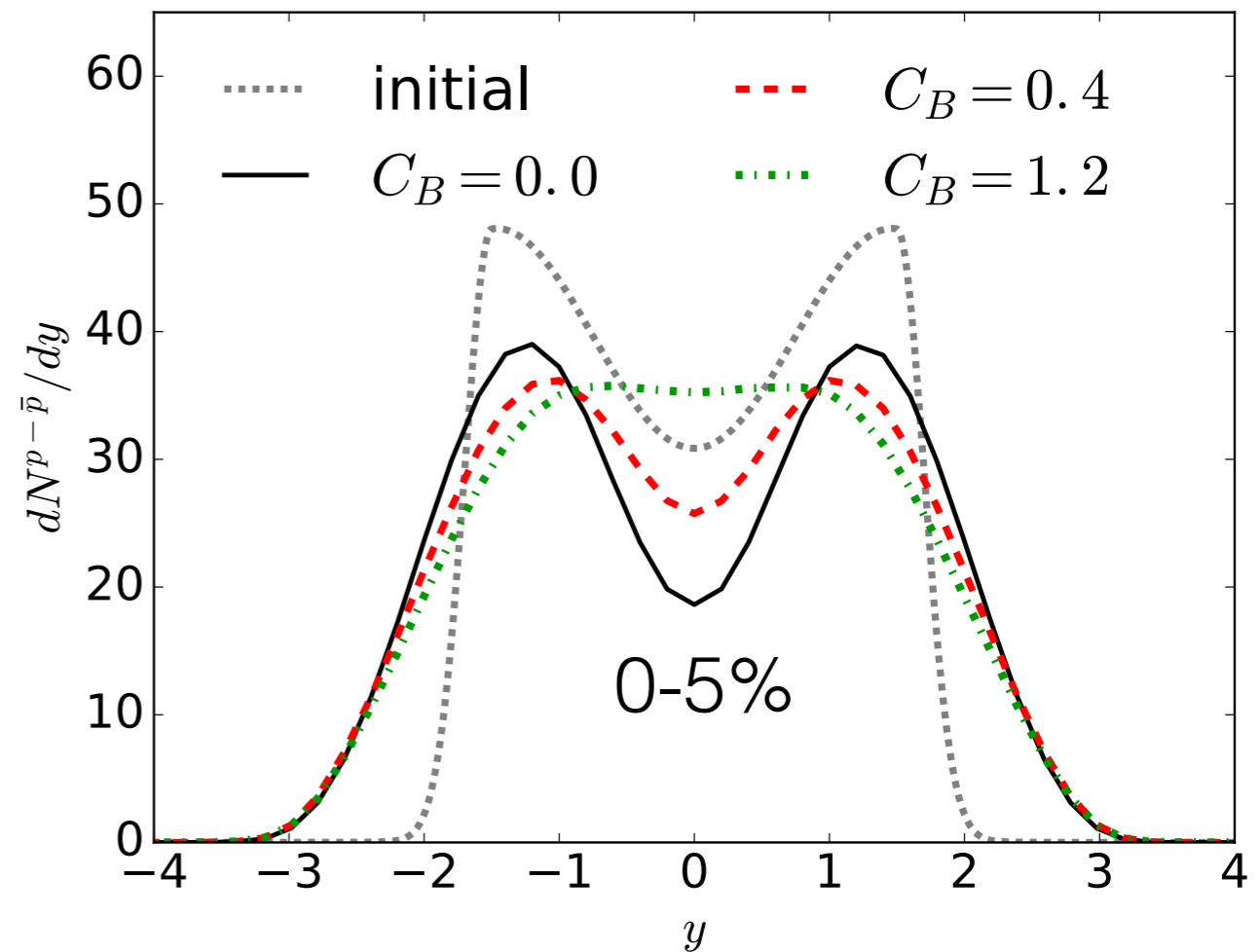
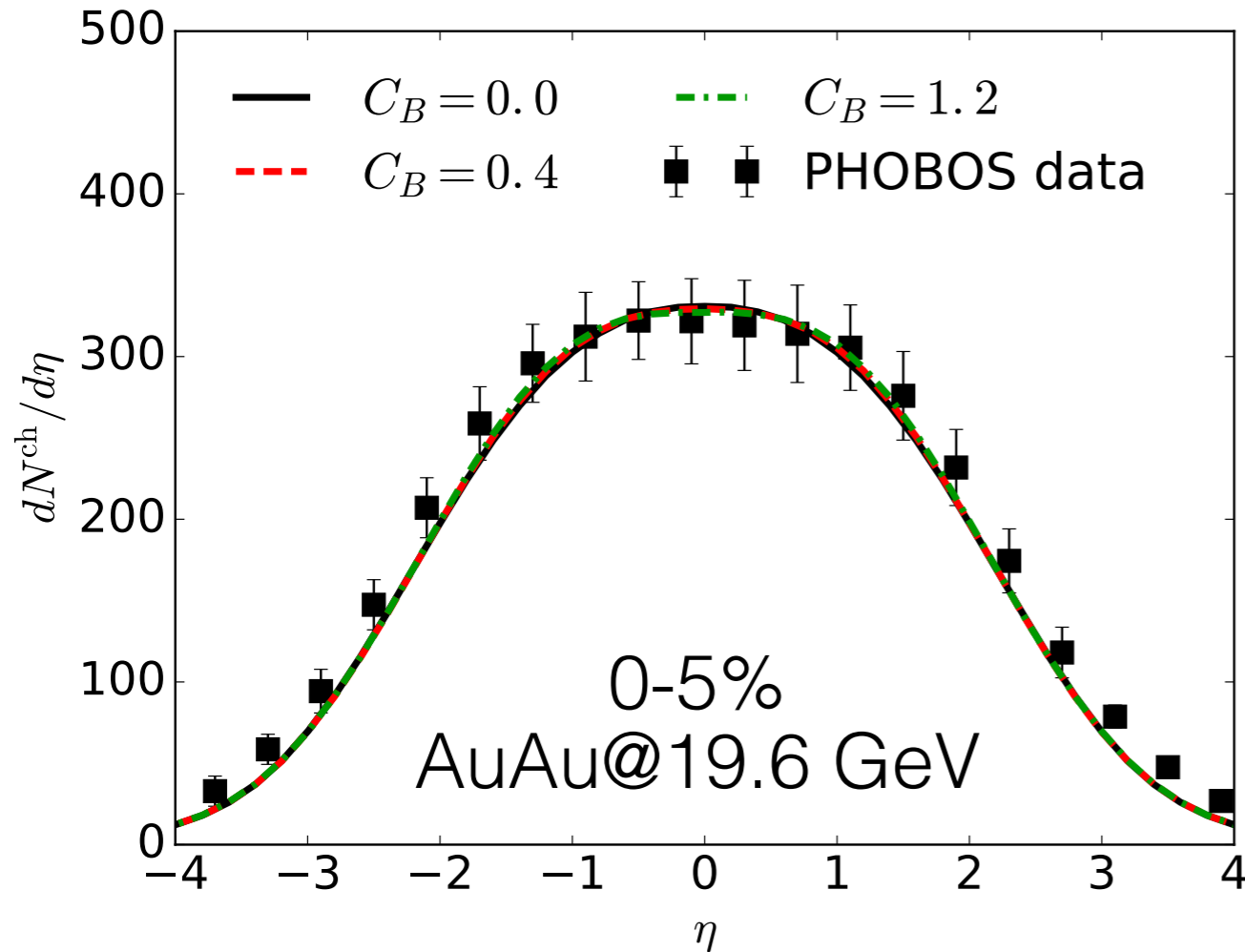
The holographic Einstein-Maxwell-Dilation (EMD) model is fit to the lattice results on thermodynamic quantities at $\mu_B = 0$

Predictions are made for thermodynamic variables at finite μ_B and for the temperature and μ_B dependence of various transport coefficients



Effects of net baryon diffusion on particle yields

C. Shen, G. Denicol, C. Gale, S. Jeon, A. Monnai, B. Schenke, in preparation



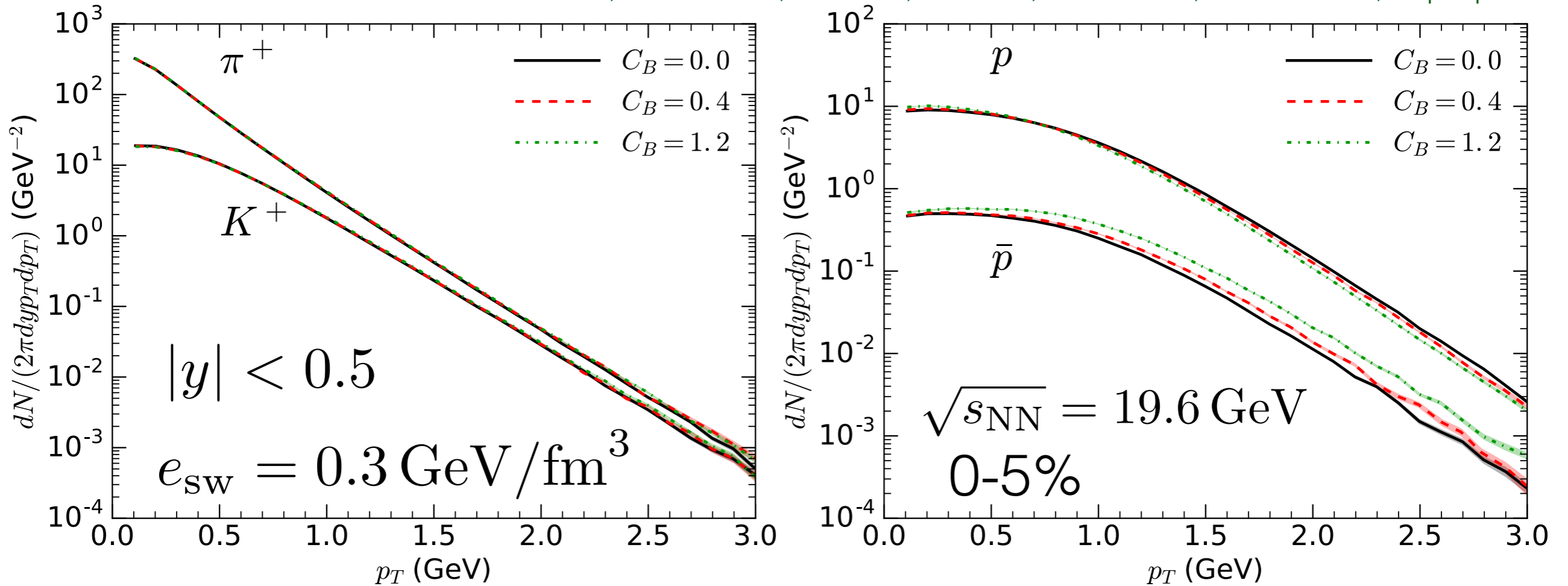
$$\kappa_B = \frac{C_B}{T} \rho_B \left(\frac{1}{3} \coth \left(\frac{\mu_B}{T} \right) - \frac{\rho_B T}{e + P} \right)$$

- More net baryon numbers are transported to mid-rapidity with a larger diffusion constant

Constraints on net baryon diffusion and initial condition

Effects of net baryon diffusion on pid spectra

C. Shen, G. Denicol, C. Gale, S. Jeon, A. Monnai, B. Schenke, in preparation



- Net baryon diffusion results a flatter spectra for anti-proton compared to proton's

	$C_B = 0.0$	$C_B = 0.4$	$C_B = 1.2$
$\langle p_{\perp} \rangle^{\bar{p}} - \langle p_{\perp} \rangle^p$ (GeV)	0.046	0.091	0.158

Stochastic Hydrodynamics

C. Young, J. Kapusta, C. Gale, S. Jeon and B. Schenke, Phys. Rev. C 91, 044901 (2015)

Treat thermal noise as perturbation

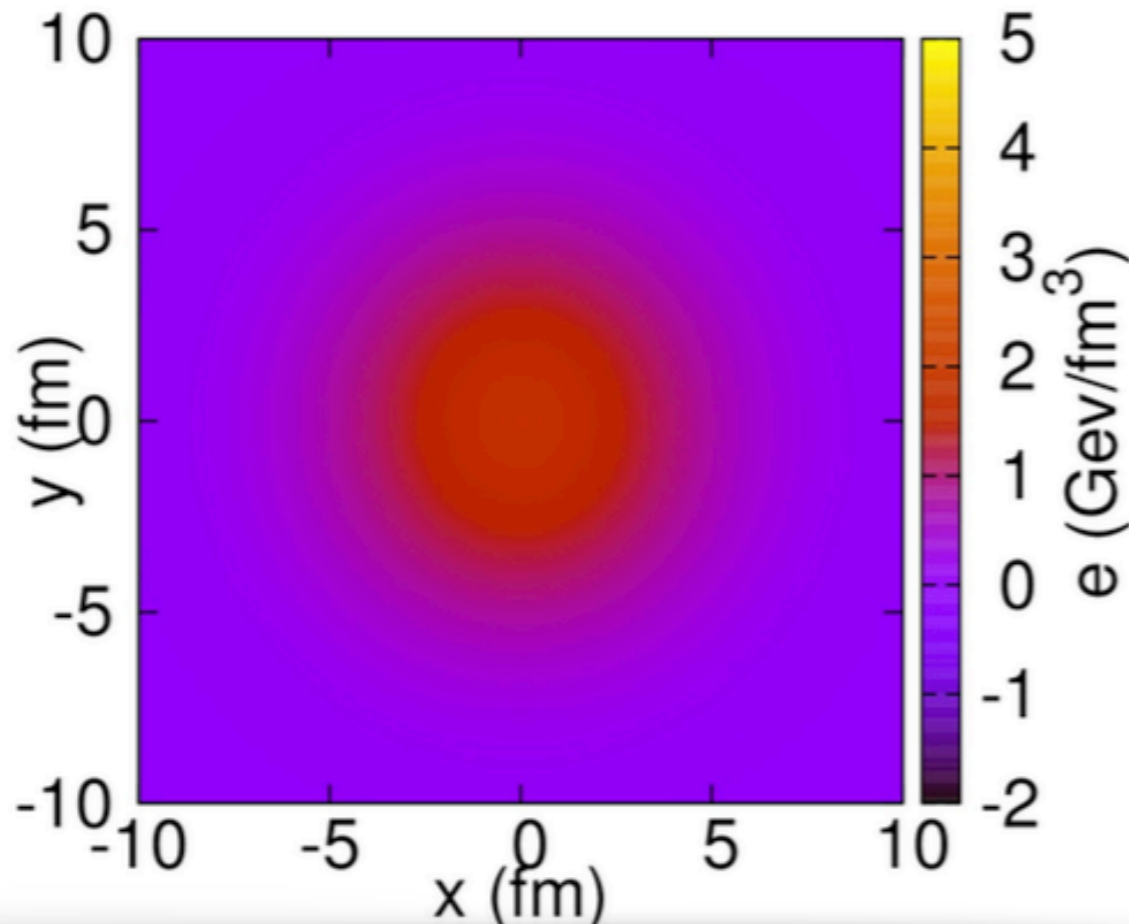
Mayank Singh

$$\partial_\mu (T_{\text{ideal}}^{\mu\nu} + \delta T^{\mu\nu} + \pi^{\mu\nu} + \delta\pi^{\mu\nu} + \Xi^{\mu\nu}) = 0$$

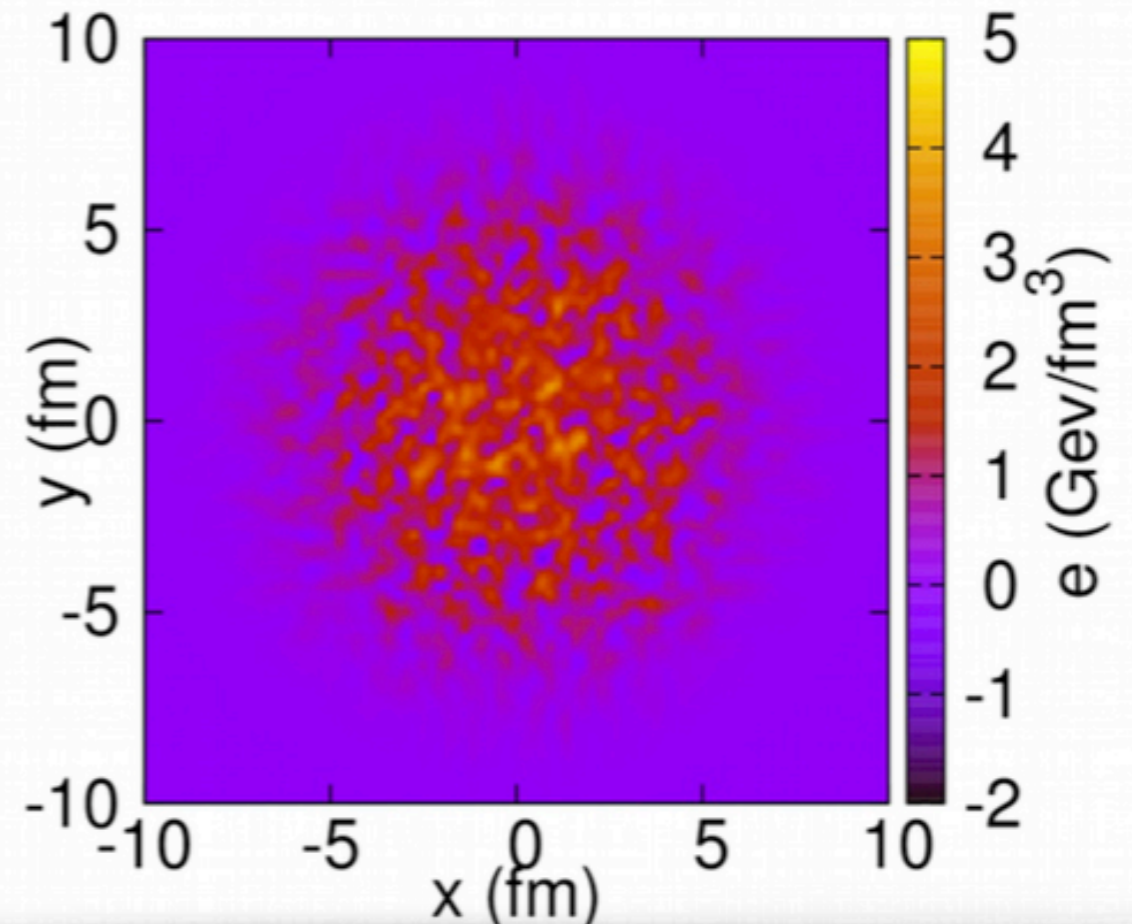
ideal fluctuation Shear fluctuation Stochastic noise



no noise

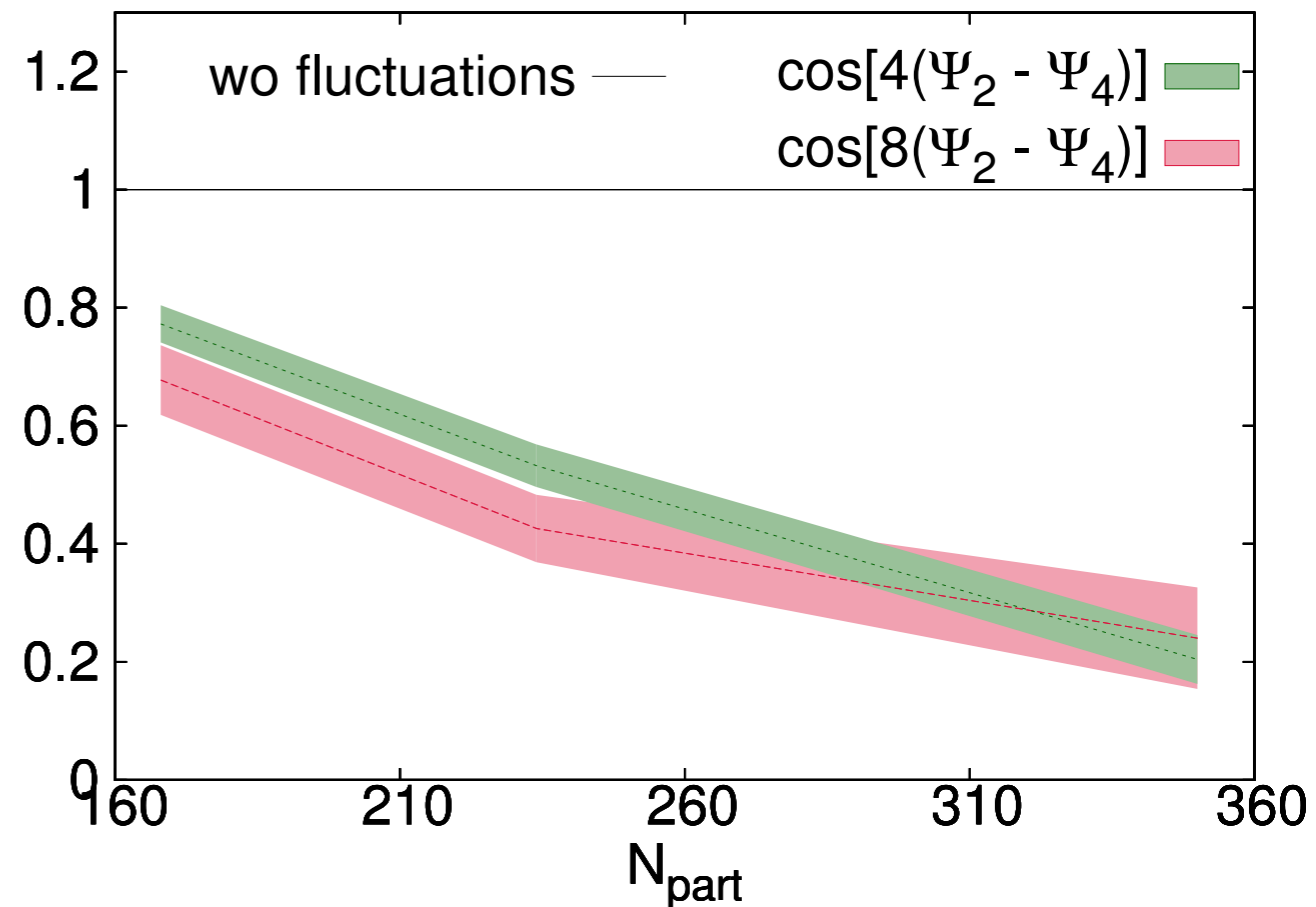
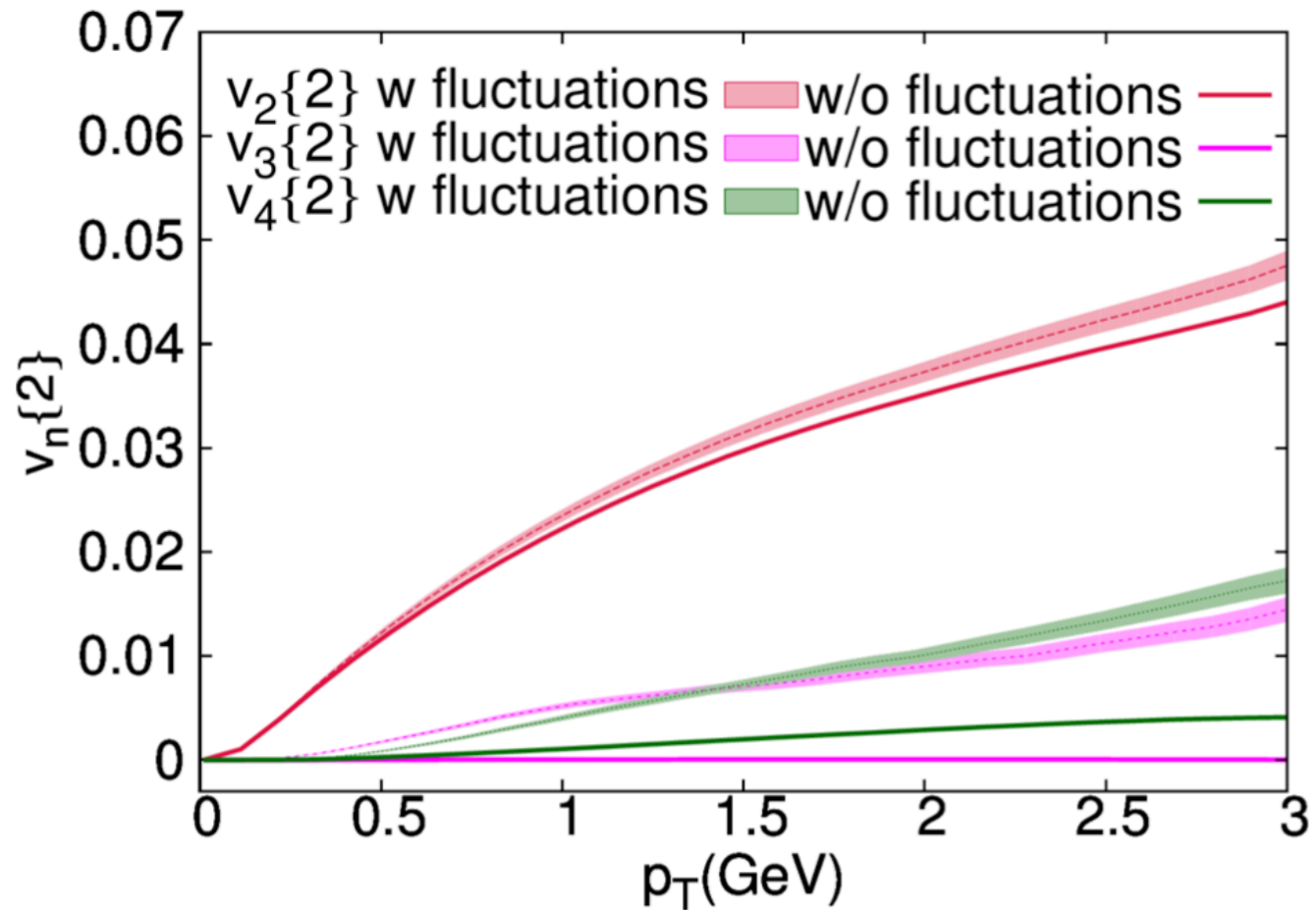


with noise



Stochastic Hydrodynamics

Mayank Singh preliminary



- The scalar product $v_n(p_T)$ increases with thermal fluctuation; Higher order v_n shows stronger sensitivity
- Thermal fluctuation reduces the correlation between different orders of event-plane angles

A more systemic approach is under way

Conclusion

- We develop a **dynamical initialization** model to study the early time evolution of heavy-ion collisions at the BES energies
 - full **(3+1)-d** event-by-event with **net baryon current**
- We identified a few experiment observables that could constrain the **net baryon diffusion**

$$dN^{p-\bar{p}}/dy \quad \langle p_{\perp} \rangle^{\bar{p}} - \langle p_{\perp} \rangle^p$$

- *Thermal fluctuation* is coupled to hydrodynamic evolution to study its impact on hadronic observables